Heliyon 9 (2023) e21880

Contents lists available at ScienceDirect

Heliyon

journal homepage: www.cell.com/heliyon

Advantages and disadvantages of treatment of experimental ARDS by M2-polarized RAW 264.7 macrophages

A.M. Kosyreva [a,b], P.A. Vishnyakova [a,c], I.S. Tsvetkov [b], V.V. Kiseleva [a,c], D. Sh. Dzhalilova [a,b,*], E.A. Miroshnichenko [a,b], A.V. Lokhonina [a,c], O.V. Makarova [b], T.H. Fatkhudinov [a,b]

[a] *Research Institute of Molecular and Cellular Medicine, Peoples' Friendship University of Russia named after Patrice Lumumba (RUDN), 6 Miklukho-Maklaya Street, 117198, Moscow, Russia*

[b] *Avtsyn Research Institute of Human Morphology of Petrovsky National Research Centre of Surgery, 3 Tsyurupy Street, 117418, Moscow, Russia*

[c] *National Medical Research Center for Obstetrics, Gynecology and Perinatology named after Academician V.I. Kulakov of Ministry of Healthcare of Russian Federation, 4 Oparina Street, 117997, Moscow, Russia*

ARTICLE INFO

Keywords:
Macrophage
ARDS
Therapy
Polarization
Lung
Immune system
Inflammation
LPS

ABSTRACT

Innate immunity reactions are core to any immunological process, including systemic inflammation and such extremes as acute respiratory distress syndrome (ARDS) and cytokine storm. Macrophages, the key cells of innate immunity, show high phenotypic plasticity: depending on microenvironmental cues, they can polarize into M1 (classically activated, pro-inflammatory) or M2 (alternatively activated, anti-inflammatory). The anti-inflammatory M2 macrophage polarization-based cell therapies constitute a novel prospective modality. Systemic administration of 'educated' macrophages is intended at their homing in lungs in order to mitigate the pro-inflammatory cytokine production and reduce the risks of 'cytokine storm' and related severe complications. Acute respiratory distress syndrome (ARDS) is the main mortality factor in pneumonia including SARS-CoV-associated cases. This study aimed to evaluate the influence of infusions of RAW 264.7 murine macrophage cell line polarized towards M2 phenotype on the development of LPS-induced ARDS in mouse model. The results indicate that the M2-polarized RAW 264.7 macrophage infusions in the studied model of ARDS promote relocation of lymphocytes from their depots in immune organs to the lungs. In addition, the treatment facilitates expression of M2-polarization markers *Arg1*, *Vegfa* and *Tgfb* and decreases of M1-polarization marker *Cd38* in lung tissues, which can indicate the anti-inflammatory response activation. However, treatment of ARDS with M2-polarized macrophages didn't change the neutrophil numbers in the lungs. Moreover, the level of the Arg1 protein in lungs decreased throughout the treatment with M2 macrophages, which is probably because of the pro-inflammatory microenvironment influence on the polarization of macrophages towards M1. Thus, the chemical polarization of macrophages is unstable and depends on the microenvironment. This adverse effect can be reduced through the use of primary autologous macrophages or some alternative methods of M2 polarization, notably siRNA-mediated.

* Corresponding author. Research Institute of Molecular and Cellular Medicine, Peoples' Friendship University of Russia named after Patrice Lumumba (RUDN), 6 Miklukho-Maklaya Street, 117198, Moscow, Russia.

E-mail address: juliajal93@mail.ru (D.Sh. Dzhalilova).

https://doi.org/10.1016/j.heliyon.2023.e21880
Received 14 February 2023; Received in revised form 20 September 2023; Accepted 31 October 2023
Available online 1 November 2023

1. Introduction

Acute respiratory distress syndrome (ARDS) is the main mortality factor in pneumonia including SARS-CoV-associated cases [1–4]. In intensive care units, ARDS is 30–50 % lethal even with advanced protocols applied to such patients [4].

Innate immunity reactions are core to any immunological process, including systemic inflammation and such extremes as acute respiratory distress syndrome (ARDS) and cytokine storm [5]. Macrophages, the key cells of innate immunity, show high phenotypic plasticity: depending on microenvironmental cues, they can polarize into M1 (classically activated, pro-inflammatory) or M2 (alternatively activated, anti-inflammatory). The microbial component lipopolysaccharide (LPS) can drive macrophage polarization to the M1 phenotype while IL-4 can induce macrophage polarization to M2 [6]. M1 macrophages are capable of pro-inflammatory responses and produce pro-inflammatory related factors such as IL-6, IL-12 and TNF. In contrast, M2 macrophages are capable of anti-inflammatory responses, repair damaged tissues and produce arginase (Arg-1) and TGF-β [7,8]. In tissues affected by infection, firstly the polarization of macrophages to pro-inflammatory M1 phenotype takes place in order to provide defense from pathogens. On the next step they are polarized to form an anti-inflammatory response to the M2 phenotype and provide the repair to damaged tissues. The regulation of macrophages polarization to provide their particular immune function was recently successfully stimulated. A key aspect of macrophage polarization is the alteration of cell surface marker expression. M1 macrophages overexpress CD38, CD80, CD86, and CD16/32, and M2 macrophages – CD163 and CD206. Changes in the balance of M1/M2 macrophages in various pathological conditions, such as tumors and inflammation, play a key role in the outcome of the disease [9,10].

The violation of the endothelial and epithelial barriers in traumas, burns, pneumonias and sepsis [11,12] leads to increased permeability of the air-blood barrier, increased migratory capacity of pulmonary neutrophils/macrophages and increased production of pro-inflammatory cytokines in the lungs [13,14]. Patients with SARS-CoV-2-associated ARDS develop the monocyte/macrophage hyperactivation and 'cytokine storm' [15] with intermediate/non-classical blood monocytes producing high amounts of IL-6 and TNF-α, which indicates the predominance of pro-inflammatory (M1) macrophage polarization. High rates of interferon production and bone-marrow macrophage infiltration have been correlated with severity of ARDS in SARS- [16,17] and MERS- [18] CoV-associated cases.

No pathogenetic treatment for ARDS is available as yet. The symptomatic options include mechanical ventilation, neuromuscular blockers, systemic corticosteroids and inhaled vasodilators [19]. Candidate biology-based strategies include the M1-to-M2 macrophage reprograming already being considered for a broad spectrum of autoimmune, proliferative and inflammatory disorders [20–24], qualified as promising in several preclinical models of ARDS [25–30].

The anti-inflammatory M2 macrophage polarization-based cell therapies constitute a novel prospective modality [31]. Systemic administration of 'educated' macrophages is intended at their homing in lungs in order to mitigate the pro-inflammatory cytokine production and reduce the risks of 'cytokine storm' and related severe complications.

There are some approaches for modelling human ARDS in laboratory animals, including intranasal administration of Staphylococcal enterotoxin-B (SEB) and intratracheal administration of lipopolysaccharide (LPS, endotoxin) [32,33]. LPS, endotoxin — the highly immunogenic cell-wall component of Gram-negative bacteria [34–37]. The intervention has a major impact on pulmonary microcirculation, causing neutrophil infiltration of respiratory units and intra-alveolar edema entailing 'cytokine storm' and reactive oxygen species outburst, critically affecting the airway and gas exchange functionalities and highly lethal [37–41]. The local inflammatory reaction is triggered by LPS binding to TLR-4 at the pulmonary epithelium surface, which stimulates the NF-κB-dependent production of pro-inflammatory cyto-/chemokines including TNF-α, IL-1, IL-6 and notably MCP-1, a crucial attractant of mononuclear leukocytes to interalveola [42]. Thus, the intratracheal LPS administration provides a feasible model of human ARDS to be used for the validation of potential influence of M2-polarized macrophages on the pulmonary inflammation deployment.

This study aimed to evaluate the influence of systemic infusions of anti-inflammatory polarized macrophages on the development of LPS-induced ARDS in mouse model. The most suitable source of mouse macrophages for ARDS treatment can be their bone marrow precursors or blood monocytes. Due to the difficulty of obtaining and the small volume of blood from mice, we chose the mouse macrophage cell line RAW 264.7 as a cell therapeutic agent, which was established from a tumor in a male mouse induced with the Abelson murine leukemia virus. This approach was also used in a number of other works [43,44]. In current work RAW 264.7 murine macrophage cell line was polarized towards M2 phenotype for activation of its anti-inflammatory phenotype and we studied the effectiveness of this treatment in LPS-induced mouse model of ARDS.

2. Materials and methods

2.1. Animals

The study was carried out on 20 adult male C57Bl/6 mice 18–20 g body weight. The animals were obtained from Stolbovaya breeding facilities (Moscow region, Russia). The animals were randomly distributed into four groups: control group (n = 5), non-treated ARDS (n = 5), RAW 264.7 macrophage-treated ARDS (non-polarized, ARDS + M, n = 5), M2-polarized macrophage-treated ARDS (ARDS + M2, n = 5). The animals were kept in an acclimatized room with conventional environmental conditions. All animals were kept in polypropylene cages (5 mice per cage) in temperature (20 ± 2 °C) and humidity (40–60 %) controlled rooms under reversed light/dark cycles (12/12 h). Mice were fed with commercial pellets (PK-120-1; Laboratorsnab LLC, Russia) and water ad libitum. All manipulations with animals were carried out according to ARRIVE guidelines and the EU Directive 2010/63/EU on the protection of animals used for scientific purposes. All efforts were made to minimize the suffering and distress of animals. Permission was obtained from the Bioethical Committee at Avtsyn Research Institute of Human Morphology (Protocol No. 21, March 29, 2019).

2.2. Cell cultures

RAW 264.7 cells were cultured in complete medium (RPMI supplemented with 10 % heat-inactivated fetal bovine serum (FBS), 2 mM L-glutamine, 25 U/mL penicillin, 25 μg/ml streptomycin (all by PanEco, Russia) in 6-well cell-culture plates (Costar, USA) at a density of 0.5×10^6 cells per well).

2.3. In vitro polarization of RAW 264.7 macrophage

RAW 264.7 cells were grown to monolayers in 175 cM^3 Corning flasks (Corning Inc., USA) with RPMI 1640 full growth medium (PanEco) containing FBS (HyClone, USA), penicillin/streptomycin (PanEco) and L-glutamine (PanEco). During polarization, the cells were incubated in full growth medium supplemented with IL-4 (50 ng/ml) for 24 h, detached, washed in PBS, centrifuged at 300 g for 5 min and counted [45].

2.4. ARDS modeling

ARDS was modeled in C57Bl/6 mice (n = 15) by intratracheal administration of 125 μL LPS *E.coli* O111:B4 (Sigma, USA) at a 15 mg/kg [46–48]. Animals of the treatment group (ARDS + M2, n = 5) received 5×10^6 of M2-polarized RAW 264.7 cells [49–51] in PBS, 300 μL intravenously, immediately post-LPS. Animals of the comparison group received identical injections of non-polarized RAW 264.7 cells (ARDS + M, n = 5). Animals of the non-treated group (ARDS, n = 5) received sham injections of 300 μL saline immediately post-LPS. Animals of the control group (Control, n = 5) received saline only — 125 μL intratracheally and 300 μL intravenously (sham-operated). The animals were withdrawn from the experiment by diethyl ether overdose administered 24 h post-intervention and right lungs, thymuses, spleens and livers were collected. Fresh tissue fragments of the lung were placed in RNAprotect Tissue Reagent (Qiagen, Germany) to preserve mRNA or snap-frozen in liquid N_2 to preserve proteins for molecular study; the rest specimens were fixed and processed for histology.

2.5. Labeling of macrophages with PKH26

RAW 264.7 cells were detached, washed in PBS, centrifuged at 300 g for 5 min, counted and stained with PKH26 dye (Sigma, PKH26GL-1 KT) according to manufacturer's protocol. After inactivation of reaction by adding 2 ml of FBS cells were centrifuged and injected intravenously in 300 μL of saline in amount of 5×10^6.4 and 24 h after the injection of PKH26-labeled RAW 264.7, the lung, liver, spleen and kidney were taken, snap-frozen in liquid N2, cryosections were prepared, cell nuclei were stained with DAPI (Thermo Fisher Scientific, P36941). The presence of PKH26-labeled RAW 264.7 was assessed under a Leica DM 4000 B microscope with sotfware LAS AF v.3.1.0 build 8587 (Leica Microsystems, Germany).

2.6. Histopathology

The lungs were fixed in Carnoy's fluid; the thymuses, the spleens and the livers were fixed in Bouin's fluid. The specimens were alcohol-dehydrated, paraffin-embedded, sectioned, mounted, stained routinely with H&E (BioVitrum, Russia) and microscopically examined. Neutrophils infiltrating interalveolar septa were counted in a standard visual area of 25,000 μm^2 [52,53]. To assess for fibrin, lungs were stained with MSB (Martius-Scarlett-Blue) according to the instructions (Biochemmack, Russia).

2.7. Immunohistochemistry

Immunohistochemical detection of M2 macrophages marker – CD206 was carried out by sandwich method. Lungs sections were deparaffinized, demasked in citrate buffer pH 6.0 with 0.5 % Tween-20 at 100 °C and blocked in phosphate-buffered saline with 0.1 % bovine serum albumin at room temperature before exposure to antibodies (primary: Rabbit Polyclonal Anti-CD206 Antibody, ab64693, Abcam, UK; secondary HRP Donkey-*anti*-Rabbit antibodies 1:500; 416035, Novex Life Technologies). After PBS cleansing, DAB work solution was amplified until color changing visualized.

2.8. Reverse transcription—polymerase chain reaction assay (RT-PCR)

Total RNA was isolated with QIAZOL reagent and RNeasy Plus Mini Kit (Qiagen) in accordance with the manufacturer's protocols; cDNA was synthesized with MMLV-RT kit (Evrogen, Russia). PCRs were set in triplicates with qPCRmix-HS SYBR master mixes (Evrogen, Russia) and target-specific primers designed using Primer-BLAST tool (NCBI, USA) and custom-ordered from Evrogen. Gene expression was quantified by threshold cycle (Ct) approach [42] against *Gapdh* as housekeeping reference target. The genes of interest were Arg*1, Il10 and Tgfb* in cultured cells and *Tnfa*, *Nos2*, *Cd38,* Arg*1*, *Vegfa* and *Tgfb* in lung tissues.

2.9. Enzyme-linked immunosorbent assay (ELISA)

The blood serum was collected from jugular veins [54]. Levels of LPS and IL-1β were measured using commercial kits (Cloud-Clone, USA) in accordance with the manufacturer's protocols.

2.10. Western blot assay

RAW 264.7 cells were lysed in RIPA buffer, mixed with 2× loading buffer (Bio-Rad, USA) and incubated at 95 °C for 1 min prior to loading. Snap-frozen tissue samples were homogenized in Protein Solubilization Buffer (Bio-Rad) using MicroRotofor Lysis Kits with the addition of Complete Protease Inhibitor Cocktail (Roche, Switzerland). Homogenized samples were centrifuged at 14,000 g for 30 min; the supernatant was collected, mixed with 2× loading buffer and incubated at 95 °C for 1 min prior to loading. The proteins were separated by 10%–12.5 % SDS-PAGE and transferred to PVDF membranes by semi-wet method using a Trans-Blot® Turbo™ RTA Mini LF PVDF Transfer Kit (Bio-Rad). The membranes were blocked with 5 % milk in Tris-buffered saline containing 0.1 % Tween for 1 h at room temperature, then incubated with primary antibodies (Arginase: sc-18351, Santa-Cruz; GAPDH: Cat.#5G4, Hytest; CD206: ab64693, Abcam; TGFbeta: ab66043 Abcam) overnight at 4 °C with gentle shaking. Next day, the membranes were incubated with HRP-conjugated secondary antibodies (Bio-Rad) for 1 h at room temperature. The bands were stained using Novex ECL Kit (Invitrogen™ Thermo Fisher Scientific, USA) and visualized in ChemiDoc MP visualization system with Image Lab Software (Bio-Rad), GAPDH used as a reference protein to measure optical density of the bands of interest. Normalization was carried out as follows: bands corresponding to individual lanes with applied samples were automatically detected in Image Lab Software, then the value of adjusted volume (the background-adjusted volume) was calculated. The corresponding value for the GAPDH band was taken as 100 %, while the signal from the protein of interest from the same sample was calculated as a fraction of it.

2.11. Statistics

Statistical analysis involved data normality tests using Kolmogorov–Smirnov method in Statistica 8.0 (StatSoft, USA) and nonparametric multiple comparison procedures using Kruskal–Wallis test. At $p < 0.05$, the differences were treated as statistically significant and Dunn's post-hoc test was applied to specify the significance for each pair. For graphical representation, the data were converted to boxplots comprising the median, IQR and upper/lower extreme values.

3. Results

3.1. M2 polarization of RAW264.7 cultures

M2 polarization of RAW 264.7 cells was induced by addition of purified recombinant IL-4 to the growth medium. The effect was tested by Arg*1* expression analysis at mRNA and protein levels, using RT-PCR and Western blot, respectively. After 24 h exposure to IL-4, the cultures expressed Arg*1* at significantly higher levels compared with non-treated controls (Fig. 1A and B). Also we analyzed expression level of another two anti-inflammatory markers: TGF-β and IL-10 (Fig. 1B) and found that *Tgf*-β expression was significantly up-regulated after IL-4 exposure while in case of *Il-10* the significant difference was not achieved. Both IL-4-treated and non-treated

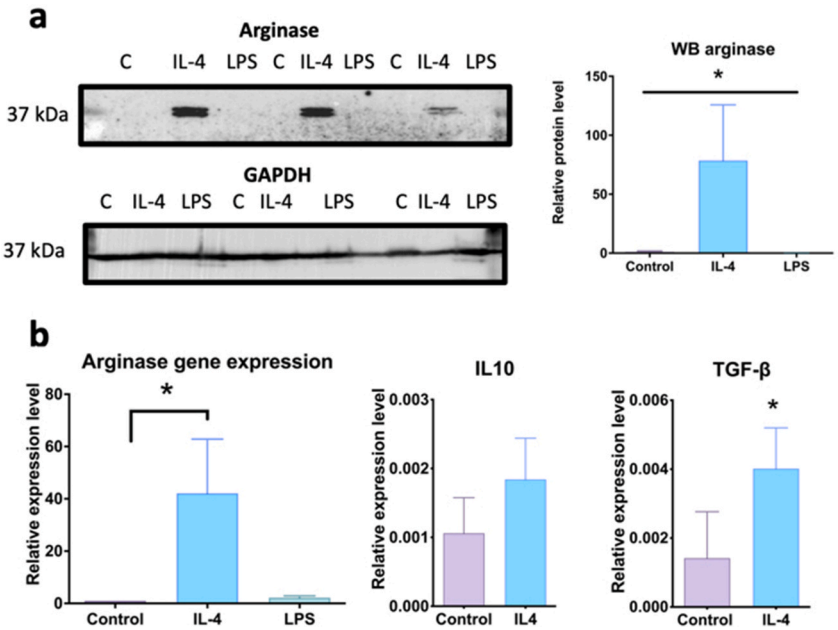

Fig. 1. Expression of *Arg1*, *Il-10 and Tgf*-β in RAW 264.7 cells after M1 and M2 polarization induced by LPS and IL-4, respectively. Representative western blots with arginase 1 signal quantitation (**A**). Relative transcription levels of Arg*1, Il-10 and Tgf-b* measured by RT-PCR (**B**). C, non-induced cells; GAPDH, reference; * — $p < 0.05$. Full-length, non-adjusted and uncroppted membranes are available in Supplementary Material.

cells were subsequently administered to C57Bl/6 mice with induced ARDS. Another negative control, LPS-treated cultures, had Arg*1* expression levels similar to non-treated cultures, indicating specificity of the IL-4-mediated induction.

3.2. Histopathology of the lungs

Histological study of lung tissues in sham-controls (no LPS and no cells administered) revealed unobstructed bronchi and clear, aerated alveoli occasionally containing eosinophilic masses, with thin septa (Fig. 2A and B). Twenty-four hours after LPS injection there was thickening of alveolar septae with accumulation of neutrophils, macrophages and lymphocytes in the lungs (Fig. 2F). In the lumen of part of the alveoli, focal accumulations of neutrophils, intraalveolar edema represented by eosinophilic masses with erythrocytes, and proteinaceous alveolar fluid and debris were noted (Fig. 2C, E). Among the cells of the inflammatory infiltrate, MSB staining revealed microthrombi and fibrin deposits (Fig. 2D). There was focal bronchopneumonia with granular eosinophilic masses in secondary and tertiary bronchi, containing disintegrating aggregated neutrophils, solitary macrophages and detached epithelial cells in the lungs (Fig. 2F).

Mice receiving LPS combined to RAW 264.7 cell infusions developed similar characteristic signs of ARDS with bronchitis and interstitial pneumonia, complemented by the appearance of broad, muff-shaped lymphocyte accumulations in perivascular spaces of pulmonary veins absent in the non-treated ARDS and control groups (Fig. 3A–D).

The migration of the introduced RAW 264.7 into the lungs, liver, kidney, and spleen was assessed by labeling the cells with the PKH vital dye. As shown in Fig. 4 both 4 h and 24 h after intravenous administration, macrophages were found in the lungs (Fig. 4A and B) and liver (Fig. 4C and D). In the spleen, macrophages were detected only 4 h after administration (Fig. 4E and F), and in the kidney, they were practically not detected at both studied periods (Fig. 4H and G).

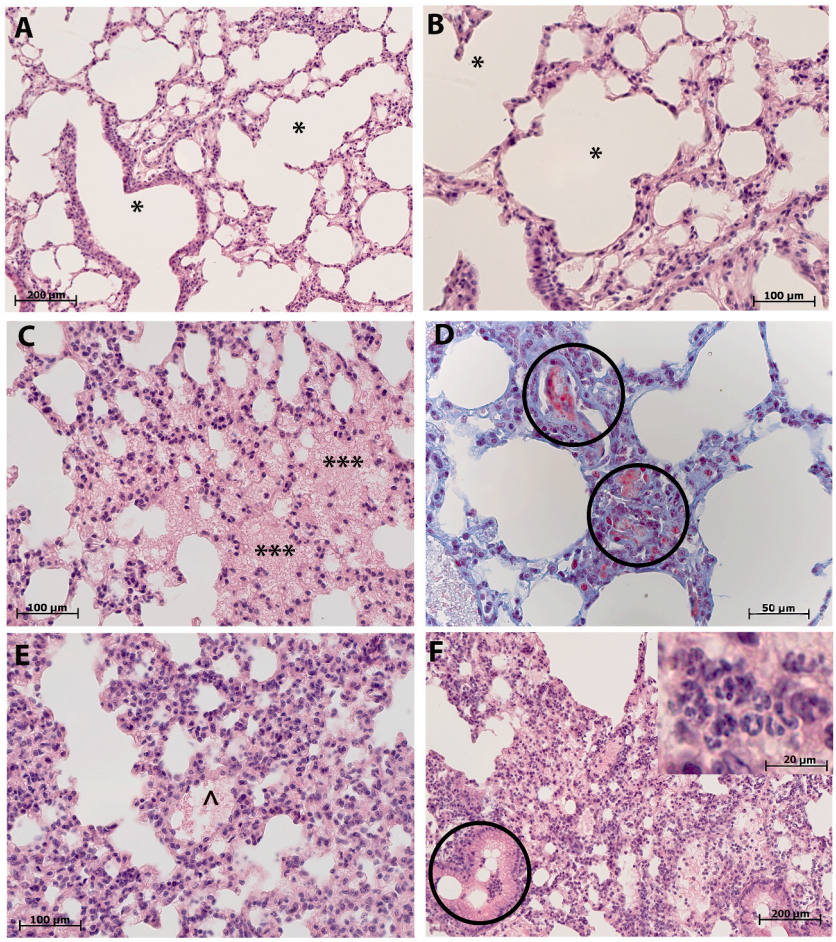

Fig. 2. Histological images of lungs in sham-controls (A, B) and non-treated ARDS (C–F). Staining — H&E (A-C, E-F), MSB (D). A, B - normal lungs structure, the alveoli are airy (*), the interalveolar septa are thin, contain single neutrophils. C - focal intraalveolar edema (***), represented by eosinophilic masses, among which erythrocytes are detected. D - fibrin deposits (circle) in the lumen of the blood vessel and interalveolar septa E – proteinaceous alveolar fluid and debris in the lumen of the alveoli (^) F - focal bronchopneumonia (circle), accumulations of neutrophils in the lumen of the bronchi (insert).

When staining the lungs with antibodies to CD206, the marker M2 of macrophages, they were detected in all the studied groups (Fig. 5A–F). In sham-operated mice, single CD206+ macrophages were found in the intraalveolar septa (Fig. 5A). Whereas, in ARDS, their number increased in the foci of inflammation, they were found in thickened interalveolar septa (Fig. 5B). When non-polarized RAW 264.7 macrophages was administered, the number of CD206+ cells was comparable to the control group (Fig. 5A and C). During therapy with polarized M2 RAW 264.7, the number of CD206+ macrophages at a qualitative level was higher than during therapy with non-polarized cells (Fig. 5D, E, F).

The degree of interstitial inflammation was quantitatively assessed by neutrophil counts within interalveolar septa. Compared to the control group, a statistically significant increase in the number of neutrophils in the interalveolar septa was found only in ARDS + M mice. However, as can be seen in Fig. 6, the number of neutrophils was higher in all experimental groups compared to the control. Thus, the morphological assessment revealed no significant differences in the severity of inflammatory changes with regard to the treatment.

3.3. Serum IL-1β and LPS

Animals with M2 macrophage-treated ARDS had lower serum levels of IL-1β (Fig. 7A) indicating a decrease in systemic inflammatory reaction compared to non-treated ARDS. Serum levels of LPS in the three groups were similar (Fig. 7B).

3.4. Cytokine expression in the lungs

Molecular study of the pulmonary inflammatory reaction involved RT-PCR for macrophage polarization markers *Nos2*, *Tnf*-α, *Cd38, Arg1*, *Vegfa* and *Tgf*-β; the data are plotted in Fig. 8. While M1 markers *Nos2, Tnf*-α and *Cd38* were expressed similarly in all groups M2 markers *Arg1*, *Vegfa* and *Tgf*-β were expressed at higher levels in animals with macrophage-treated ARDS than in the non-treated ARDS and control groups, with the most pronounced effect observed for M2-polarized cell treatment. Worth noting that mRNA of M1 macrophages marker *Cd38* decreased in both macrophage-treated ARDS groups regardless of their polarization.

3.5. Arg1, CD206 and TGF-β expression in the lungs

Next, we analyzed the production of typical M2 markers in lung tissue after treatment of the ARDS model by Western blotting. We observed overall down-regulation of Arg1 in all ARDS groups but the significant difference was achieved in case of ARDS + M (Fig. 9).

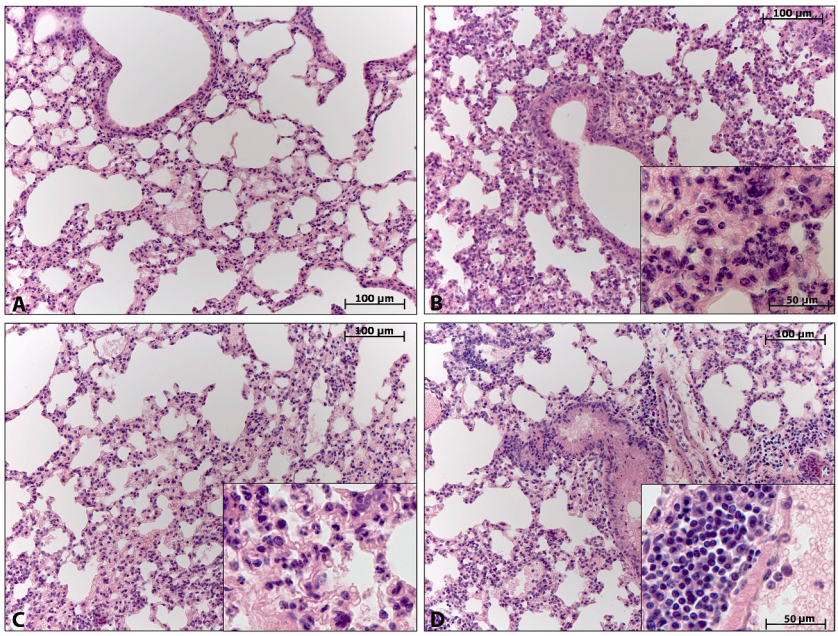

Fig. 3. Representative histological images of right lung parenchyma in sham-controls (**A**), non-treated ARDS (**B**) and RAW 264.7 macrophage-treated ARDS (non-polarized, ARDS + M, **C**; M2-polarized, ARDS + M2, **D**). Staining — H&E. **A.** Normal microanatomy: bronchi unobstructed; alveoli clear, occasionally with eosinophilic masses, with thin septa. **B.** Characteristic signs of pulmonary inflammation with infiltrated septa; the insert shows neutrophil aggregations. **C.** Characteristic signs of pulmonary inflammation with infiltrated septa; the insert shows mixed infiltrate containing neutrophils, lymphocytes and macrophages. **D.** Characteristic signs of pulmonary inflammation, septa infiltrated with neutrophils, lymphocytes and macrophages; the insert shows muff-shaped lymphoid accumulations around pulmonary veins, with solitary neutrophils and macrophages.

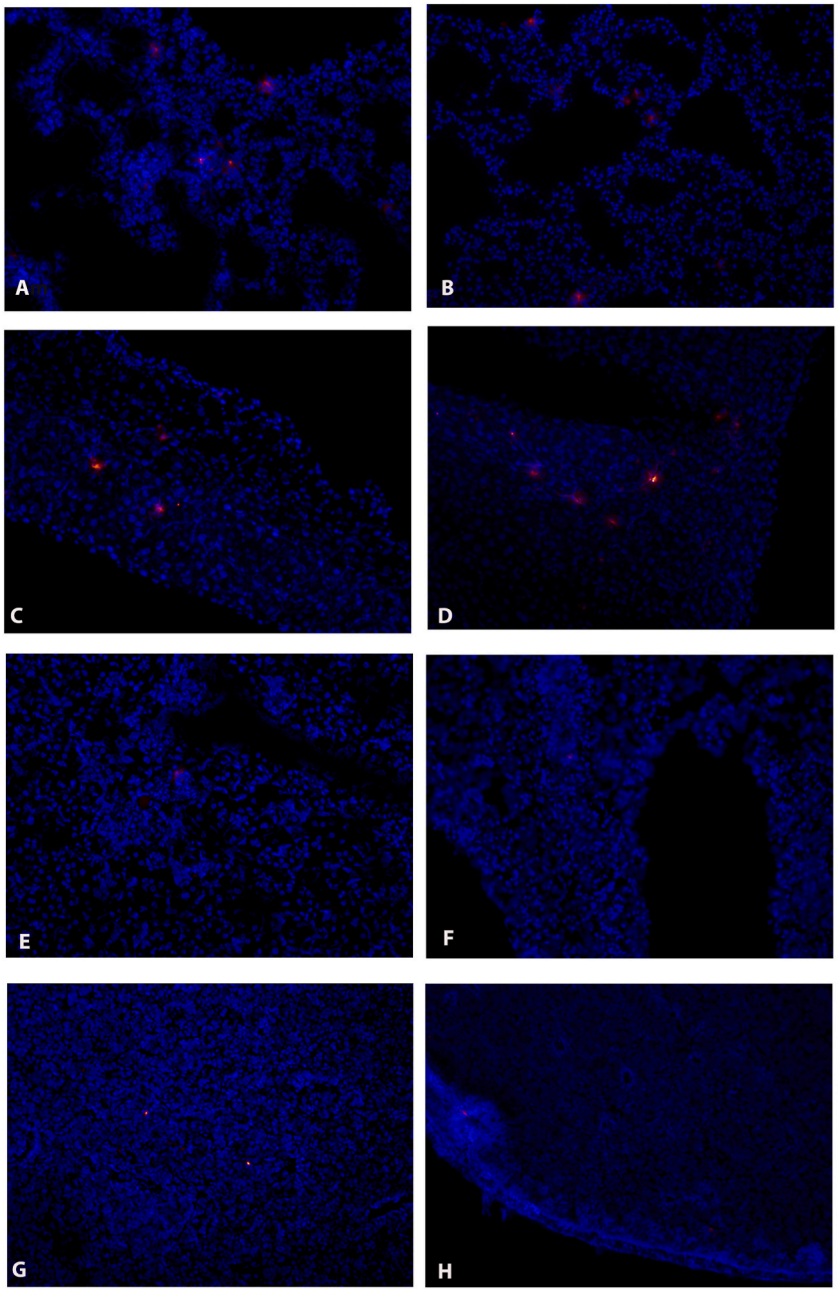

Fig. 4. Distribution of PKH-labeled RAW264.7 in lungs (A, B), liver (C, D), kidney (E, F), and spleen (G, H) at 4 h (A, C, E, G) and 24 h (B, D, F, H) after intravenous administration to mice. Magnification - ×200.

Also we found a significant decrease of CD206 expression in M2-polarized cell treated ARDS compared to control group. Interestingly, the level of TGF-β was down-regulated in ARDS + M and ARDS + M2 animals but the difference was not significant.

3.6. Histopathology of thymus, spleen and liver

Non-autologous cell transplantations may entail significant immunological burden and thereby affect the thymus and the spleen, as well as the liver. We carried out histopathological assessment for possible changes in these organs with regard to the treatment, for all groups of the study.

Histopathological study of the thymus in the control and non-treated ARDS groups revealed typical zonality with distinct cortico-medullary boundaries (Fig. 10A and B), the cortex densely populated with lymphocytes. In animals with non-polarized macrophage-

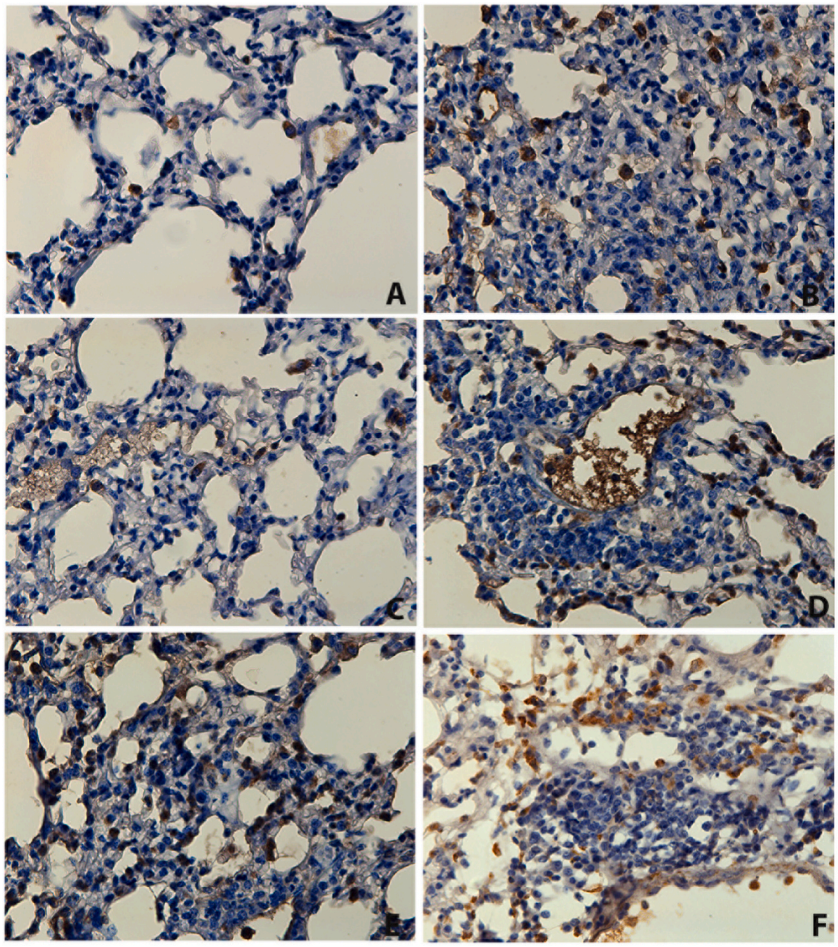

Fig. 5. CD206+ M2 macrophages in the lungs of control mice (A), ARDS (B) and RAW 264.7 macrophage-treated ARDS (non-polarized, ARDS + M, C; M2-polarized, ARDS + M2, D-F). Staining - ICH with antibodies to CD206. Magnification - ×400.

treated ARDS, the thymus had characteristic 'starry sky' appearance indicating death of thymocytes, with prominent macrophages scavenging the debris (Fig. 10C); the picture was complemented by neutrophil-infiltrated cyst-like cavities in the medulla characteristic of ongoing accidental involution [43]. Animals with M2-polarized macrophage-treated ARDS had advanced thymic involution with massive death of thymocytes, formation of apoptotic bodies in the cortex and neutrophil-/macrophage-infiltrated cavities in the medulla (Fig. 10D).

Compared to the normal splenic architecture observed in the control group (Fig. 11A), animals with non-treated ARDS presented with enlarged germinal centers of splenic follicles and decreased counts of cellular elements in the red pulp most probably reflecting the intensified migration of immune cells to the inflamed areas in the lungs (Fig. 11B). Animals with ARDS receiving non-polarized RAW 264.7 cells had splenic morphology similar to animals with non-treated ARDS (Fig. 11C). Animals with ARDS receiving M2-polarized RAW 264.7 cells presented with signs of white pulp depletion and decreased counts of splenic follicles (Fig. 11D) indicative of higher lymphocyte expenditure; the red pulp contained observable accumulations of neutrophils, lymphocytes and histiocytes (Fig. 11D).

Compared to the normal liver architecture observed in the control group (Fig. 12A), the liver in non-treated ARDS presented with medium-droplet hepatocyte dystrophy, affecting about 30 % of the cells predominantly at the periphery of the lobules (Fig. 12B). In non-polarized macrophage-treated ARDS, the dystrophy was less pronounced (Fig. 12C); M2-polarized macrophage injections promoted higher counts of non-epithelial cellular elements in the lobules, while mitigating hepatocyte dystrophy (Fig. 12D).

4. Discussion

In our work, we have chosen the chemical method of macrophage polarization as a proven and reliable approach, which has also been used in a huge number of *in vitro* studies [55–58]. Upon IL-4 exposure, RAW 264.7 macrophages acquired M2-like phenotypes, as indicated by elevated expression/production levels of arginase 1 — the M2 marker enzyme responsible for arginine conversion into ornithine and urea [59–61,]. In murine macrophages, *Arg1* expression can be induced by PGE_2, Th2 cytokines and cAMP [61]; the

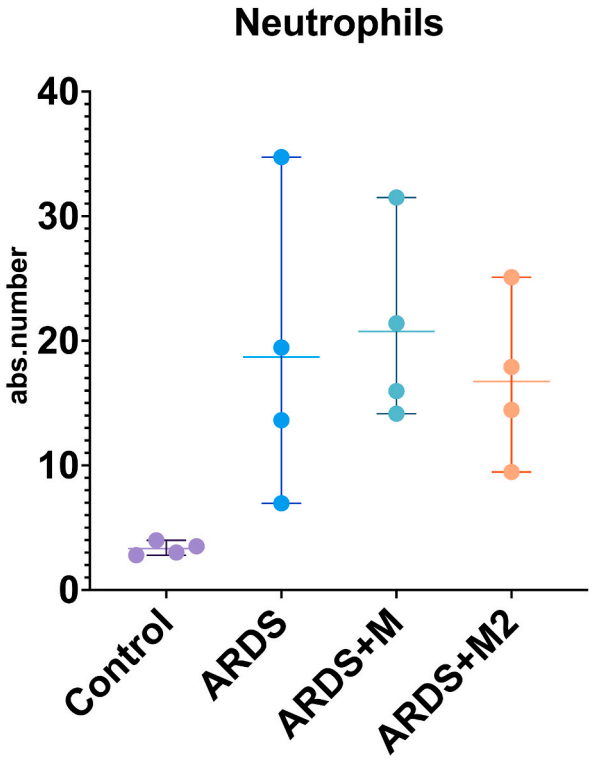

Fig. 6. Absolute neutrophils number in interalveolar septa of the lungs counted in a standard visual area of 25,000 μm^2 in health (**Control, n = 5**), non-treated ARDS (**ARDS, n = 5**) and ARDS treated with RAW 264.7 macrophages (non-polarized, **ARDS + M, n = 5**; M2-polarized, **ARDS + M2, n = 5**). Kruskal–Wallis test, Dunn's method.

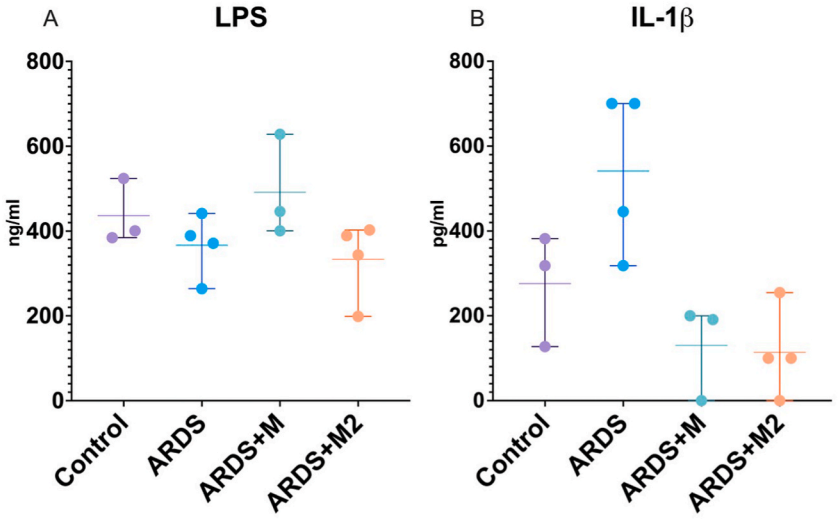

Fig. 7. Serum levels of LPS (**A**) and IL-1β (**B**) in sham-controls (**Control, n = 5**), non-treated ARDS (**ARDS, n = 5**) and RAW 264.7 macrophage-treated ARDS (non-polarized, **ARDS + M, n = 5**; M2-polarized, **ARDS + M2, n = 5**). Kruskal–Wallis test, Dunn's method.

induction mediated by STAT-6 and CEBP/b binding to IL-4 response element in *Arg1* promoter has been demonstrated in RAW 264.7 cell line [62,63]. The anti-inflammatory 'healing' effects of M2-polarized macrophages involve the arginase pathway as the means for both detoxication of arginine as the NOS substrate and production of anti-inflammatory ornithine derivatives [59]. The anti-inflammatory properties of arginase-expressing macrophages have been demonstrated in murine schistosomiasis model; the mechanisms involve IL-12/IL-23 synthesis suppression and maintenance of favorable Treg/Th17 balance [64,65].

Our morphometric data reveal no alleviation of the inflammatory reaction in response to the treatment, notably the lack of

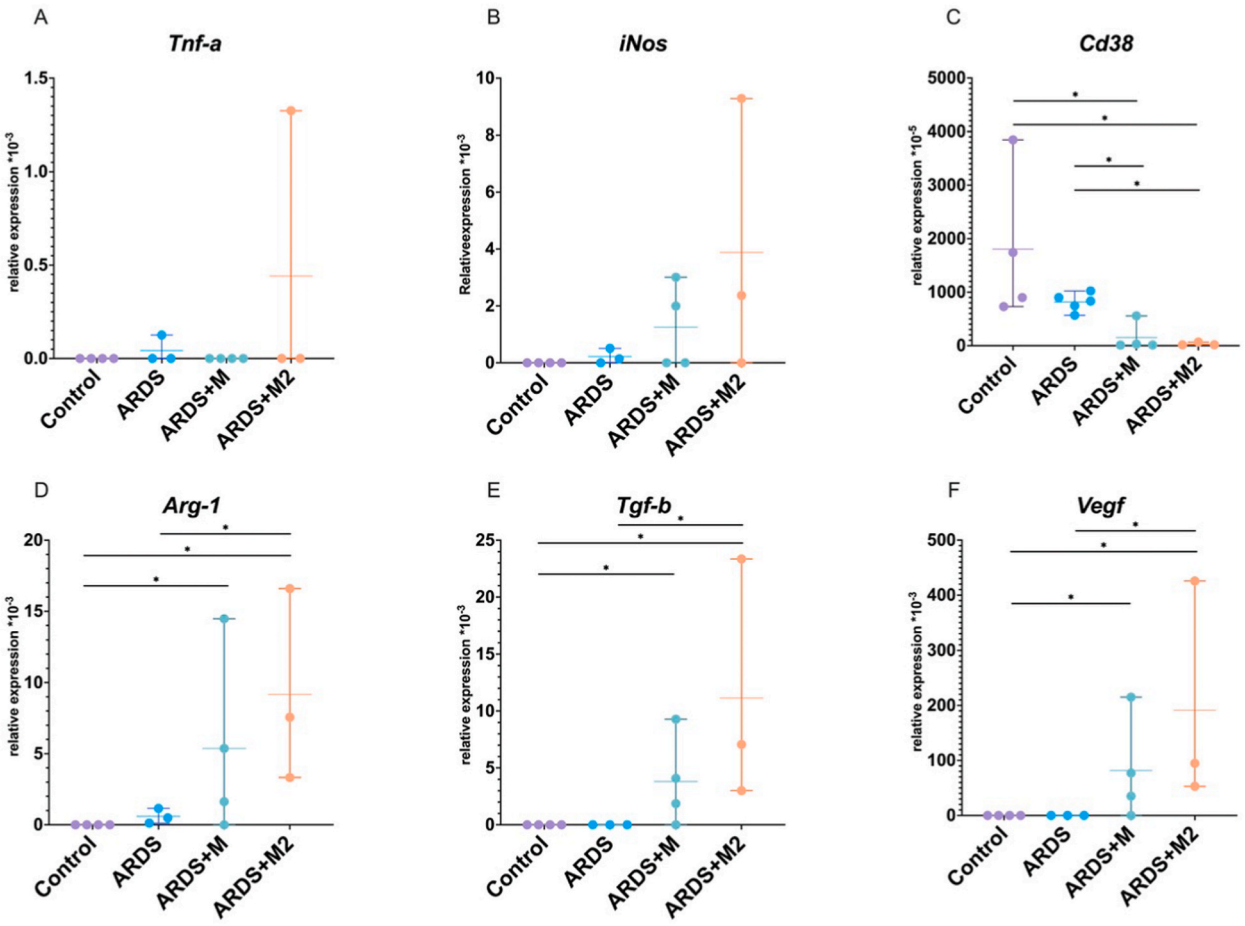

Fig. 8. Relative mRNA expression levels of *Tnf*-α (**A**), *Nos2* (**B**), *Cd38* (**C**), *Arg1* (**D**), *Tgf*-β (**E**) and *Vegf*α (**F**) in the lungs in sham-controls (**Control, n = 5**), non-treated ARDS (**ARDS, n = 5**) and RAW 264.7 macrophage-treated ARDS (non-polarized, **ARDS + M, n = 5**; M2-polarized, **ARDS + M2, n = 5**). Kruskal–Wallis test, Dunn's method.

significant differences in septal neutrophil counts as compared with the non-treated control group. The lack of morphologically evident response can be attributed to the temporary nature of the chemically induced macrophage polarization. Upon their arrival in the lungs, the RAW 264.7-M2 cells become exposed to the LPS-conditioned milieus of distinctly pro-inflammatory character, facilitating a reverse shift towards M1. However, we didn't reveal an increase of expression level of M1 marker - Cd38, that can be activated by LPS [10]. In both groups of ARDS treatment we found a decrease of *Cd38* expression. This could be the result of inhibition of LPS-induced polarization of M1 macrophages [66]. Moreover, CD38 expresses on the surface of various immune cells, not only in macrophages, but in regulatory T cells (Tregs), regulatory B cells (Bregs), myeloid-derived suppressor cells (MDSCs) and $CD16^{-}CD56^{+}$ natural killer (NK) cells [67,68]. The increase of CD38 is observed in many inflammatory and cancer diseases [69–72] and targeted CD38 therapy would be a promising treatment for a variety of diseases [68]. In addition, according to the IHC study, more CD206+ macrophages were detected in the lungs during treatment with M2-type polarized RAW 264.7 than without treatment and during therapy with non-polarized RAW 264.7. CD206, also known as mannose receptor C type 1 (MRC1), is a cell-surface protein abundantly presents on selected populations of dendritic cells and macrophages [73]. CD206 is normally expressed on the M2 but not M1 macrophage subtype and therefore serves as a useful marker to identify the M2 phenotype.

The validation of anti-inflammatory effects of polarized macrophages carried out by us in this study was confined to a single time-point of 24 h post-intervention, which is perhaps suboptimal for the morphologically evident response in the lungs. Still, we observed significant molecular-level effects of the treatment in terms of transcriptomic changes, including increased expression of *Arg1*, *Vegfa* and *Tgf*-β. Increased expression of the arginase-encoding gene *Arg1* is indicative of M2 macrophage polarization [74]. *Arg1* expression by alveolar macrophages can support the airway remodeling through increased production of L-ornithine as a biochemical precursor for L-proline (used in collagen synthesis) and polyamines putrescine, spermidine and spermine [75]. *Arg1* expression by endothelial cells promotes an increase in capillary permeability through decreased production of NO [76]; accordingly, the increased expression of *Arg1* in lung tissues of the M2 macrophage-treated mice with induced ARDS could favor neutrophil infiltration of the septa and promote the lymphocyte aggregation in perivascular spaces of pulmonary veins. On the other hand, introduction of *in vitro/ex vivo* polarized macrophages expressing M2 signatures could promote a similar M2 polarization in both alveolar and recruited macrophages

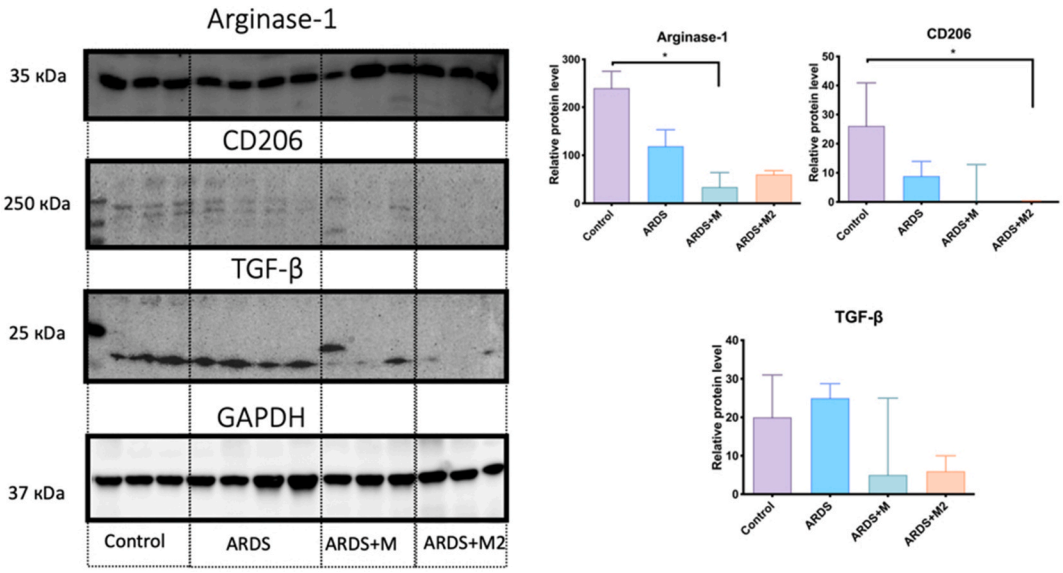

Fig. 9. Western blot analysis of protein expression in lung tissue in sham-controls (Control, **n = 3**), non-treated ARDS (ARDS, **n = 4**) and RAW 264.7 macrophage-treated ARDS (non-polarized, ARDS + M, **n = 3**; M2-polarized, ARDS + M2, **n = 3**). Representative western blotting membranes stained with antibodies to Arginase 1, CD206, TGF-β and GAPDH. Relative expression levels of Arg1, CD206 and TGF-β, normalized by GAPDH level. * - $p < 0.05$. Full-length, non-adjusted and uncroppted membranes are available in Supplementary Material.

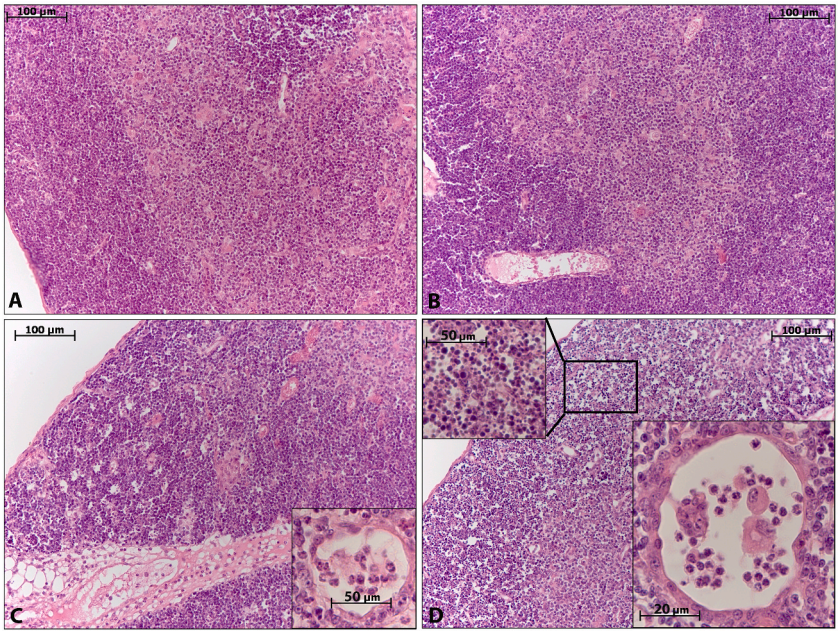

Fig. 10. Representative histological images of the thymus in in sham-controls (**A**), non-treated ARDS (**B**) and RAW 264.7 macrophage-treated ARDS (non-polarized, ARDS + M, **C**; M2-polarized, ARDS + M2, **D**). Staining — H&E. Magnification — × 200, inserts × 400, × 640. **A, B.** Normal microanatomy: cortex densely populated with thymocytes, clear cortico-medullary boundaries. **C.** 'Starry sky' patterns with prominent macrophages scavenging non-viable thymocytes in the cortex and neutrophil-infiltrated cyst-like cavities in the medulla. **D.** Advanced accidental thymic involution: massive lymphocyte death, neutrophil-/macrophage-infiltrated cyst-like cavities in the medulla.

at the pulmonary inflammation foci. The level of the Arg1 protein in lungs decreased throughtout the treatment with M2 macrophages, which is probably because of the pro-inflammatory microenvironment influence on the polarization of macrophages towards M1. This results suggest the primitiveness of M1/M2 paradigm. Modern data demonstrate that even in the lack of polarizing stimuli, the macrophage phenotype is heterogeneous and exists in a continuum [77]. Moreover, the continuum of macrophages' plasticity provides itself as in physiological and pathological conditions. These states, for which there is a lack of clear manifesting signs of the M1 or M2

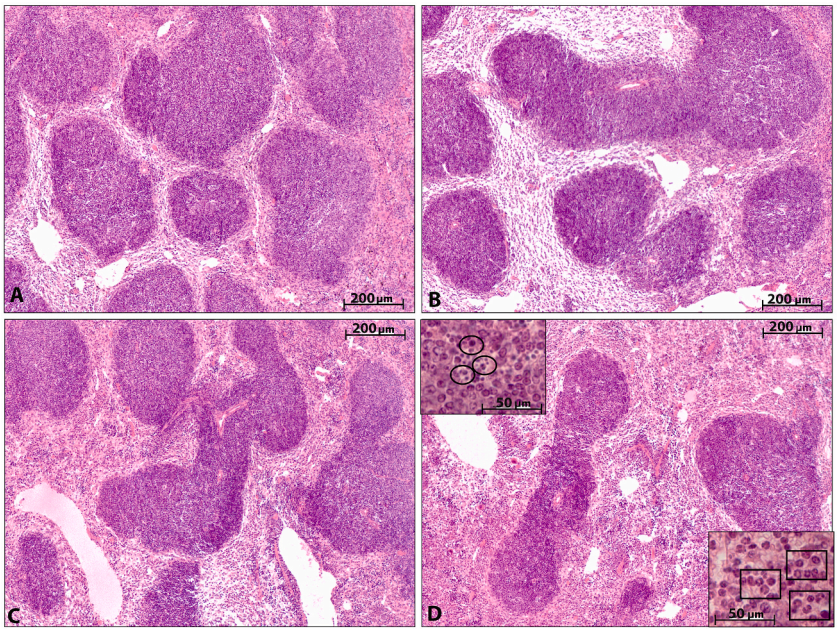

Fig. 11. Representative histological images of the spleen in in sham-controls (**A**), non-treated ARDS (**B**) and RAW 264.7 macrophage-treated ARDS (non-polarized, ARDS + M, **C**; M2-polarized, ARDS + M2, **D**). Staining — H&E. Magnification — × 100, inserts × 640. **A.** Normal splenic microanatomy: white pulp composed of lymphoid follicles with non-enlarged central areas. **B, C.** Enlarged germinal centers of splenic follicles, red pulp depleted of cellular elements. **D.** White pulp depletion, red pulp myelosis with focal accumulations of lymphocytes and neutrophils (in rectangles) or their fragments (in ovals).

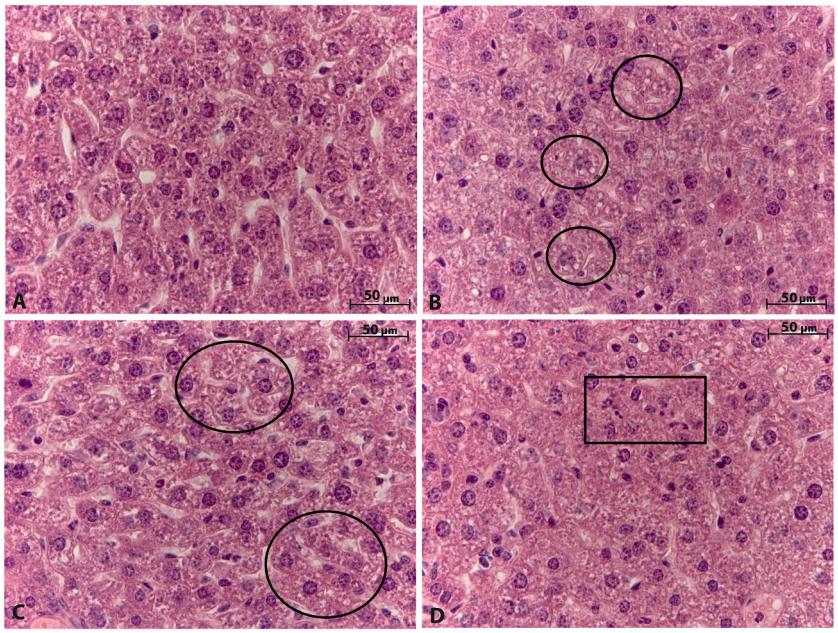

Fig. 12. Representative histological images of the liver in in sham-controls (**A**), non-treated ARDS (**B**) and RAW 264.7 macrophage-treated ARDS (non-polarized, ARDS + M, **C**; M2-polarized, ARDS + M2, **D**). Staining — H&E. Magnification — × 640. **A.** Normal microanatomy: hepatocytes without dystrophic changes, containing glycogen inclusions. **B.** Medium-droplet hepatocyte dystrophy (circles). **C.** Small-/medium-droplet hepatocyte dystrophy (circles). **D.** Increased counts of non-epithelial cellular elements in the lobules, notably neutrophils (square).

phenotype correspond in literature to the so-called hybrid phenotypes [78]. Now it is postulated that the M1/M2 paradigm reflects the *in vitro* extremization of the *in vivo* conditions. Despite the criticism, many authors who publish works relating to macrophages still reference the M1/M2 paradigm, even in recently published works [79–83].

In addition, the level of CD206, estimated by the WB method, decreased with both M and M2 RAW 264.7 therapy, however, in the IHC study, on the contrary, the expression of CD206+ cells during M2 macrophage therapy was higher than in the comparison groups. This may be due to the uneven distribution of CD206+ macrophages in the lungs in ARDS: for example, they were found in areas of thickening of the intraalveolar septa and in areas of lymphocytic muffs surrounding the veins. Whereas the material for WB is taken "blindly" and it is impossible to predict the zone of the lungs with pathological changes characteristic of ARDS on macropreparations.

VEGF, the key pro-angiogenic molecule, has been featured as a favorable prognostic factor in ARDS [84,85]. Increased expression of VEGF by alveolar macrophages invigorates their phagocytic activity towards apoptotic cells [86]. Also, VEGF-A has been shown to enhance the air-blood barrier permeability and thereby increase the risks of pulmonary edema [87]. The increase in transcription levels of *Vegfa* in response to the treatment with M2-polarized macrophages, revealed by us in this study, may indicate the efferocytosis activation; on the other hand, it may be correlated with increased permeability of the blood-brain barrier and the appearance of perivascular lymphoid sleeves revealed histologically.

The transforming growth factor beta (TGF-β) is known to support the post-ARDS collagen production and lung architecture re-establishment [88] through promotion of the fibroblast-to-myofibroblast transition and extracellular matrix remodeling [89,90]. Other studies find no correlation between pulmonary levels of TGF-β and proliferation of fibroblastic lineages in ARDS and hence dismiss it as a favorable marker, especially with consideration to its high expression in the lungs of patients dying of COVID-19 [89]; apparently, during the acute phase the role of TGF-β is different from its 'peaceful' contribution to the post-acute healing.

M2-polarized macrophages are known to produce TGF-β [91]; moreover, increased production of this factor by mesenchymal stem cells has been shown to support the M2 macrophage polarization [92]. The elevated expression of *Tgf-β* in the lungs revealed in our experiments may determine the subsequent onset of fibrosis while indirectly indicating M2 polarization of alveolar macrophages. However, despite the increased transcription rates of *Arg1*, *Vegfa* and *Tgf*-β in the affected lungs after treatment, no corresponding changes at the protein level were encountered during Western blot analysis.

The M2-polarized macrophage administration significantly reduced serum levels of IL-1β compared to control animals with non-treated ARDS, indicating alleviation of the inflammatory reaction at systemic level. The LPS exposure is known to promote a TLR-4-dependent activation of NF-κB pathway, resulting in boosted serum levels of pro-inflammatory IL-1β, TNF-α and IL-6, which stimulate the synthesis of acute inflammation proteins, notably CRP, by the liver [93]. High serum IL-1β is considered an adverse prognostic marker in severe SARS-CoV-2-associated ARDS [94].

The histological assessment of the immunity organs revealed distinctive signs of increased antigenic load on the thymus and the spleen in response to the treatment. Compared with other groups of the study, thymuses of mice receiving infusions of the M2-polarized RAW264.7 cells revealed significant cortical atrophy and transition of thymic bodies into cyst-like cavities subject to neutrophil infiltration. The reduced counts of lymphoid nodules in splenic white pulp indicated massive loss of lymphocytes through apoptosis and/or migration to the liver and the lungs. The latter assumption is supported by the appearance of sleeve-like immune cell aggregations in perivascular spaces of pulmonary veins and the increased counts of non-epithelial cellular elements within the liver sinusoids.

Thus, the results indicate that the M2-polarized RAW264.7 macrophage infusions in the studied model of ARDS promote relocation of lymphocytes from their depots in immune organs to the lungs, where they tend to aggregate in perivascular spaces of pulmonary veins. In addition, the treatment facilitates expression of M2-polarization markers *Arg1*, *Vegfa* and *Tgf*-β in lung tissues, which can indicate the anti-inflammatory response activation. However, when administered as early as 24 h after the induction of ARDS with LPS, the treatment fails to prevent the development of acute inflammatory reaction as measured by neutrophil counts. The histological assessment of the thymus reveals the signs of accidental involution with massive death of cortical thymocytes in response to the treatment. In the spleen, the histological assessment reveals white pulp depletion and red pulp myelosis, indicative of the strong antigenic load conferred by the allogeneic cell infusion. This adverse effect can be reduced through the use of primary autologous macrophages or some alternative methods of M2 polarization, notably siRNA-mediated.

There is a growing body of evidence of cell-based therapy effectiveness for ARDS. A great number of research and clinical trials use mesenchymal stem cells (MSCs) and MSCs-derived exosomes for ARDS treatment [95,96]. Nonetheless, low engraftment and poor survival of transplanted MSCs are the reasons for clinical translation of such therapeutic approach. MSCs can be genetically modified to overexpress beneficial genes or pre-treated with a series of preconditioning strategies, which can promote their therapeutic effects [97]. The boost of therapeutic effects may be due to the increase in the engraftment and survival of MSCs in the lung, a decrease in the oxidative pathology, and improved effects of angiogenesis, anti-inflammation, and anti-apoptosis. However viral transfection is correlated with the possibility of oncogenes and tumorigenesis triggering. Furthermore, the establishment of genetically modified MSCs is time-consuming, and it might be difficult to provide genetically modified MSCs immediately following the start of ARDS.

A series of preconditioning strategies have been developed to enhance the therapeutic capacity of MSCs in animal ARDS models, that include hypoxia conditions [98–100], pre-treatment with N-Acetylcysteine, a precursor of glutathione with anti-oxidative effect [101], pre-activation with serum obtained from ARDS patients [102], pretreatment with low levels of TGF-β1 [103].

Another way for treatment of ARDS is the using of small interfering RNAs (siRNAs) wherein siRNA may be implemented to modify the expression of pro-inflammatory cytokines and chemokines at the mRNA level [104]. This therapy could be effective because of accessibility, relative immune privilege, and relatively low enzyme activity in the lung [105]. However, its translation into the clinic is hampered by an inefficient delivery to the target cells owing to several unfavorable physicochemical properties of naked siRNA. So siRNA reprogrammed macrophages could be perspective treatment strategy for ARDS therapy [106,107]. Relevant targets for

inactivation may include microRNAs; for instance, miR-34a has been reported to facilitate M2 macrophage polarization and alleviate the LPS-induced lung injury in a Klf4-dependent manner [108]. Incidentally, the ultrashort wave (USW) therapy is likely to induce M2 macrophage polarization and thereby alleviate the inflammatory reaction, as has been demonstrated in rat model of LPS-induced acute lung injury [109].

While cell therapy has a number of benefits, it also comes with some risks. Although cell donors are extensively screened to rule out systemic illnesses and undergo screening for a panel of infectious diseases (including human immunodeficiency virus (HIV-1, HIV-2), hepatitis B, hepatitis C, human T-lymphotropic virus I/II, cytomegalovirus, and syphilis) [110], the use of cell therapy for various diseases involves the cultivation of donor cells, which is associated with the possibility of infection of the therapeutic product. In addition, the age of the donor may affect the effectiveness of therapy [111], and genetic heterogeneity, which may determine the production of effector molecules by cells [112].

The use of autologous macrophages can help to avoid these problems, but they can only be obtained in intensive care during the acute phase of the disease, which can affect the properties of macrophages and lead to ineffective therapy. In addition, blood-derived monocytes can carry viral particles, including COVID-19, and play the role of a Trojan horse. The penetration of infected monocytes through blood-tissue barriers, notably the 'Trojan horse' delivery of viral particles into the central nervous system, is common for HIV [113–115], human herpes virus [116], human cytomegalovirus [117] and Japanese encephalitis virus [118] infections. It provides stable viral pools, which are capable of sudden amplification upon optimal conditions for their reactivation [5].

Furthermore, in human population there are several types of ARDS course, such as hyperinflammatory phenotype with higher mortality and less pronounced phenotype, some disadvantages in cell therapy in ARDS may be due to individual peculiarities of patients. And the using of cell therapy for ARDS treatment in patient with hyperinflammatory immune response can be more effective than in other types. Inclusion of all patients in a clinical trial to determine efficacy of MSCs may dilute any potential signal for efficacy, reducing the effective power of a clinical study and degrading statistical power and effect size estimates of clinical studies in ARDS, reducing the power of these studies to detect important differences [110,119].

Moreover, there are a number of difficulties in applying siRNA-based therapy in clinical practice. Firstly, the usage of siRNA is time consuming, and associated with the complexity of siRNA delivery, which needs to use siRNA-conjugated antibodies or transfecting agents that often have a toxic effect on cells. In addition, knockdown of one gene with siRNA may not always help to achieve the desired polarization effect due to signaling bypass shunts.

At the moment, the concept of clinical application of *ex vivo* activated macrophages is just beginning to develop. Our study shows the promise of this direction: potentially, macrophages derived from their own blood monocytes can be used to treat diseases of various origins. The closest example to the concept of our work is cytokine-induced killer cells: T- and NK cells that are generated by *ex vivo* incubation of peripheral blood mononuclear cell with IFN-γ, anti-CD3 antibody, IL-1/IL-2 and then injected in organism at various diseases [120]. Cytokine-induced killer cells are currently serving as a cellular therapeutic agent in several clinical trials. It is likely that the development of macrophages *ex vivo* polarization with further reverse transplantation will bring us closer to their clinical use in humans. Hence, due to some limitations of M2-macrophage polarization, further investigations of macrophage-based therapy are necessary.

Ethics statement

All experimental protocols were strictly followed in accordance with the ARRIVE guidelines, and EU Directive 2010/63/EU on the protection of animals used for scientific purposes, and all the experimental protocols were carried out with the approval of the Bioethical Committee at Avtsyn Research Institute of Human Morphology (Protocol No. 21, March 29, 2019).

Author contributions

Anna Kosyreva: Conceived and designed the experiments; Performed the experiments; Analyzed and interpreted the data; Wrote the paper. Polina Vishnyakova: Conceived and designed the experiments; Performed the experiments; Analyzed and interpreted the data; Wrote the paper. Ivan Tsvetkov: Performed the experiments; Analyzed and interpreted the data; Contributed reagents, materials, analysis tools or data. Victoria Kiseleva: Conceived and designed the experiments; Analyzed and interpreted the data; Contributed reagents, materials, analysis tools or data. Dzhuliia Dzhalilova: Conceived and designed the experiments; Analyzed and interpreted the data; Wrote the paper. Ekaterina Miroshnichenko: Performed the experiments; Contributed reagents, materials, analysis tools or data. Anastasia Lokhonina: Performed the experiments; Contributed reagents, materials, analysis tools or data. Olga Makarova: Conceived and designed the experiments; Wrote the paper. Timur Fatkhudinov: Conceived and designed the experiments; Wrote the paper.

Funding

This work was supported by Russian Science Foundation [grant number 22-15-00241] and budgetary theme 123030700103-6. Work of Vishnyakova P.A. was supported by a grant for young Russian scientists MK-1573.2022.3.

Data availability statement

Data will be made available on request.

Additional information

No additional information is available for this paper.

Declaration of competing interest

The authors declare the following financial interests/personal relationships which may be considered as potential competing interests:Timur Fatkhudinov reports financial support was provided by Russian Science Foundation.

Appendix A. Supplementary data

Supplementary data to this article can be found online at https://doi.org/10.1016/j.heliyon.2023.e21880.

References

[1] J.E. Michalski, J.S. Kurche, D.A. Schwartz, From ARDS to pulmonary fibrosis: the next phase of the COVID-19 pandemic? Transl. Res. 241 (2022) 13–24, https://doi.org/10.1016/j.trsl.2021.09.001.

[2] B. Gosangi, A.N. Rubinowitz, D. Irugu, C. Gange, A. Bader, I. Cortopassi, COVID-19 ARDS: a review of imaging features and overview of mechanical ventilation and its complications, Emerg. Radiol. 29 (1) (2022) 23–34, https://doi.org/10.1007/s10140-021-01976-5.

[3] E. Fan, D. Brodie, A.S. Slutsky, Acute respiratory distress syndrome: advances in diagnosis and treatment, JAMA 319 (7) (2018) 698–710, https://doi.org/10.1001/jama.2017.21907.

[4] J. Maca, O. Jor, M. Holub, P. Sklienka, F. Burša, M. Burda, et al., Past and present ARDS mortality rates: a systematic review, Respir. Care 62 (1) (2017) 113–122, https://doi.org/10.4187/respcare.04716.

[5] A. Kosyreva, D. Dzhalilova, A. Lokhonina, P. Vishnyakova, T. Fatkhudinov, The role of macrophages in the pathogenesis of SARS-CoV-2-associated acute respiratory distress syndrome, Front. Immunol. 12 (2021), 682871, https://doi.org/10.3389/fimmu.2021.682871.

[6] A. Sica, A. Mantovani, Macrophage plasticity and polarization: in vivo veritas, J. Clin. Invest. 122 (3) (2012) 787–795, https://doi.org/10.1172/JCI59643.

[7] P.J. Murray, J.E. Allen, S.K. Biswas, E.A. Fisher, D.W. Gilroy, S. Goerdt, et al., Macrophage activation and polarization: nomenclature and experimental guidelines, Immunity 41 (1) (2014) 14–20, https://doi.org/10.1016/j.immuni.2014.06.008.

[8] L.B. Ivashkiv, Epigenetic regulation of macrophage polarization and function, Trends Immunol. 34 (5) (2013) 216–223, https://doi.org/10.1016/j.it.2012.11.001.

[9] J.L. Schultze, A. Schmieder, S. Goerdt, Macrophage activation in human diseases, Semin. Immunol. 27 (4) (2015) 249–256, https://doi.org/10.1016/j.smim.2015.07.003.

[10] K.A. Jablonski, S.A. Amici, L.M. Webb, D. Ruiz-Rosado Jde, P.G. Popovich, S. Partida-Sanchez, M. Guerau-de-Arellano, Novel markers to delineate murine M1 and M2 macrophages, PLoS One 10 (12) (2015), e0145342, https://doi.org/10.1371/journal.pone.0145342.

[11] M. Bhatia, S. Moochhala, Role of inflammatory mediators in the pathophysiology of acute respiratory distress syndrome, J. Pathol. 202 (2) (2004) 145–156, https://doi.org/10.1002/path.1491.

[12] A.N. Fahmi, G.S. Shehatou, H.A. Salem, Levocetirizine pretreatment mitigates lipopolysaccharide-induced lung inflammation in rats, BioMed Res. Int. 2018 (2018), 7019759, https://doi.org/10.1155/2018/7019759.

[13] M.A. Matthay, G.A. Zimmerman, Acute lung injury and the acute respiratory distress syndrome: four decades of inquiry into pathogenesis and rational management, Am. J. Respir. Cell Mol. Biol. 33 (4) (2005) 319–327, https://doi.org/10.1165/rcmb.F305.

[14] L.B. Ware, M.A. Matthay, The acute respiratory distress syndrome, N. Engl. J. Med. 342 (18) (2000) 1334–1349, https://doi.org/10.1056/NEJM200005043421806.

[15] D. Zhang, R. Guo, L. Lei, H. Liu, Y. Wang, Y. Wang, et al., Frontline Science: COVID-19 infection induces readily detectable morphologic and inflammation-related phenotypic changes in peripheral blood monocytes, J. Leukoc. Biol. 109 (1) (2021) 13–22, https://doi.org/10.1002/JLB.4HI0720-470R.

[16] R. Channappanavar, S. Perlman, Pathogenic human coronavirus infections: causes and consequences of cytokine storm and immunopathology, Semin. Immunopathol. 39 (2017) 529–539, https://doi.org/10.1007/s00281-017-0629-x.

[17] E. Prompetchara, C. Ketloy, T. Palaga, Immune responses in COVID-19 and potential vaccines: lessons learned from SARS and MERS epidemic, Asian Pac. J. Allergy Immunol. 38 (1) (2020) 1–9, https://doi.org/10.12932/AP-200220-0772.

[18] S. Perlman, A.A. Dandekar, Immunopathogenesis of coronavirus infections: implications for SARS, Nat. Rev. Immunol. 5 (12) (2005) 917–927, https://doi.org/10.1038/nri1732.

[19] H. Banavasi, P. Nguyen, H. Osman, A.O. Soubani, Management of ARDS - what works and what does not, Am. J. Med. Sci. 362 (1) (2021) 13–23, https://doi.org/10.1016/j.amjms.2020.12.019.

[20] Z. Huang, Y. Cai, C. Yang, Z. Chen, H. Sun, Y. Xu, et al., Knockdown of RNF6 inhibits gastric cancer cell growth by suppressing STAT3 signaling, OncoTargets Ther. 11 (2018) 6579–6587, https://doi.org/10.2147/OTT.S174846.

[21] A. Shapouri-Moghaddam, S. Mohammadian, H. Vazini, M. Taghadosi, S.A. Esmaeili, F. Mardani, et al., Macrophage plasticity, polarization, and function in health and disease, J. Cell. Physiol. 233 (9) (2018) 6425–6440, https://doi.org/10.1002/jcp.26429.

[22] K. Patel, H.J. West, Febrile neutropenia, JAMA Oncol. 3 (12) (2017) 1751, https://doi.org/10.1001/jamaoncol.2017.1114.

[23] N.R. Aggarwal, L.S. King, F.R. D'Alessio, Diverse macrophage populations mediate acute lung inflammation and resolution, Am. J. Physiol. Lung Cell Mol. Physiol. 306 (8) (2014) 709–725, https://doi.org/10.1152/ajplung.00341.2013.

[24] D. Zhou, C. Huang, Z. Lin, S. Zhan, L. Kong, C. Fang, et al., Macrophage polarization and function with emphasis on the evolving roles of coordinated regulation of cellular signaling pathways, Cell. Signal. 26 (2) (2014) 192–197, https://doi.org/10.1016/j.cellsig.2013.11.004.

[25] J. Wang, M. Zhu, J. Pan, C. Chen, S. Xia, Y. Song, Circular RNAs: a rising star in respiratory diseases, Respir. Res. 20 (2019) 3, https://doi.org/10.1186/s12931-018-0962-1.

[26] Y. Zhuo, D. Li, L. Cui, C. Li, S. Zhang, Q. Zhang, et al., Treatment with 3,4-dihydroxyphenylethyl alcohol glycoside ameliorates sepsis-induced ALI in mice by reducing inflammation and regulating M1 polarization, Biomed. Pharmacother. 116 (2019), 109012, https://doi.org/10.1016/j.biopha.2019.109012.

[27] Y. Wang, M. Zhong, Z. Wang, J. Song, W. Wu, D. Zhu, The preventive effect of antiplatelet therapy in acute respiratory distress syndrome: a meta-analysis, Crit. Care 22 (2018) 60, https://doi.org/10.1186/s13054-018-1988-y.

[28] M.I. Bittencourt-Mernak, N.M. Pinheiro, F.P. Santana, M.P. Guerreiro, B.M. Saraiva-Romanholo, S.S. Grecco, et al., Prophylactic and therapeutic treatment with the flavonone sakuranetin ameliorates LPS-induced acute lung injury, Am. J. Physiol. Lung Cell Mol. Physiol. 312 (2) (2017) 217–230, https://doi.org/10.1152/ajplung.00444.2015.

[29] G.W. Tu, Y. Shi, Y.J. Zheng, M.J. Ju, H.Y. He, G.G. Ma, et al., Glucocorticoid attenuates acute lung injury through induction of type 2 macrophage, J. Transl. Med. 15 (1) (2017) 181, https://doi.org/10.1186/s12967-017-1284-7.

[30] F.R. D'Alessio, J.M. Craig, B.D. Singer, D.C. Files, J.R. Mock, B.T. Garibaldi, et al., Enhanced resolution of experimental ARDS through IL-4-mediated lung macrophage reprogramming, Am. J. Physiol. Lung Cell Mol. Physiol. 310 (8) (2016) 733–746, https://doi.org/10.1152/ajplung.00419.2015.

[31] X. Chen, J. Tang, W. Shuai, J. Meng, J. Feng, Z. Han, Macrophage polarization and its role in the pathogenesis of acute lung injury/acute respiratory distress syndrome, Inflamm. Res. 69 (9) (2020) 883–895, https://doi.org/10.1007/s00011-020-01378-2.

[32] A. Mohammed, H.K. Alghetaa, J. Zhou, S. Chatterjee, P. Nagarkatti, M. Nagarkatti, Protective effects of Δ9 -tetrahydrocannabinol against enterotoxin-induced acute respiratory distress syndrome are mediated by modulation of microbiota, Br. J. Pharmacol. 177 (22) (2020) 5078–5095, https://doi.org/10.1111/bph.15226.

[33] H. Alghetaa, A. Mohammed, N. Singh, K. Wilson, G. Cai, N. Putluri, M. Nagarkatti, P. Nagarkatti, Resveratrol attenuates staphylococcal enterotoxin B-activated immune cell metabolism via upregulation of miR-100 and suppression of mTOR signaling pathway, Front. Pharmacol. 14 (2023), 1106733, https://doi.org/10.3389/fphar.2023.1106733.

[34] K.L. Brigham, B. Meyrick, Endotoxin and lung injury, Am. Rev. Respir. Dis. 133 (1986) 913–927.

[35] G. Matute-Bello, C.W. Frevert, T.R. Martin, Animal models of acute lung injury, Am. J. Physiol. Lung Cell Mol. Physiol. 295 (3) (2008) 379–399, https://doi.org/10.1152/ajplung.00010.2008.

[36] A.M. Kosyreva, O.V. Makarova, L.V. Kakturskiy, L.P. Mikhailova, M.N. Boltovskaya, K.A. Rogov, Sex differences of inflammation in target organs, induced by intraperitoneal injection of lipopolysaccharide, depend on its dose, J. Inflamm. Res. 11 (2018) 431–445, https://doi.org/10.2147/JIR.S178288.

[37] S. Atluri, L. Manchikanti, J.A. Hirsch, Expanded umbilical cord mesenchymal stem cells (UC-MSCs) as a therapeutic strategy in managing critically ill COVID-19 patients: the case for compassionate use, Pain Physician 23 (2) (2020) E71–E83.

[38] J. Gao, B.X. Zeng, L.J. Zhou, S.Y. Yuan, Protective effects of early treatment with propofol on endotoxin-induced acute lung injury in rats, Br. J. Anaesth. 92 (2) (2004) 277–279, https://doi.org/10.1093/bja/aeh050.

[39] R. Shen, A.B. Olshen, M. Ladanyi, Integrative clustering of multiple genomic data types using a joint latent variable model with application to breast and lung cancer subtype analysis, Bioinformatics 25 (22) (2009) 2906–2912, https://doi.org/10.1093/bioinformatics/btp543.

[40] C. Fu, X. Dai, Y. Yang, M. Lin, Y. Cai, S. Cai, Dexmedetomidine attenuates lipopolysaccharide-induced acute lung injury by inhibiting oxidative stress, mitochondrial dysfunction and apoptosis in rats, Mol. Med. Rep. 15 (1) (2017) 131–138, https://doi.org/10.3892/mmr.2016.6012.

[41] X. Hu, H. Shen, Y. Wang, M. Zhao, Liver X receptor agonist TO901317 attenuates paraquat-induced acute lung injury through inhibition of NF-κB and JNK/p38 MAPK signal pathways, BioMed Res. Int. 2017 (2017), 4652695, https://doi.org/10.1155/2017/4652695.

[42] K. Baudiß, R. de Paula Vieira, S. Cicko, K. Ayata, M. Hossfeld, N. Ehrat, et al., C1P attenuates lipopolysaccharide-induced acute lung injury by preventing NF-κB activation in neutrophils, J. Immunol. 196 (5) (2016) 2319–2326, https://doi.org/10.4049/jimmunol.1402681.

[43] B. Zhang, J. Wang, J. Gao, Y. Guo, X. Chen, B. Wang, et al., Alternatively activated RAW264.7 macrophages enhance tumor lymphangiogenesis in mouse lung adenocarcinoma, J. Cell. Biochem. 107 (1) (2009) 134–143, https://doi.org/10.1002/jcb.22110.

[44] H. Zheng, J. Li, X. Luo, C. Li, L. Hu, Q. Qiu, et al., Murine RAW264.7 cells as cellular drug delivery carriers for tumor therapy: a good idea? Cancer Chemother. Pharmacol. 83 (2) (2019) 361–374, https://doi.org/10.1007/s00280-018-3735-0.

[45] X. Bao, X. Liu, N. Liu, S. Zhuang, Q. Yang, H. Ren, et al., Inhibition of EZH2 prevents acute respiratory distress syndrome (ARDS)-associated pulmonary fibrosis by regulating the macrophage polarization phenotype, Respir. Res. 22 (2021) 194, https://doi.org/10.1186/s12931-021-01785-x.

[46] D.W.H. Riches, T.R. Martin, Overview of innate lung immunity and inflammation, Methods Mol. Biol. 1809 (2018) 17–30, https://doi.org/10.1007/978-1-4939-8570-8_2.

[47] S. Alper, J.J. William, Lung innate immunity and inflammation: methods and protocols, Methods Mol. Biol. (2018) 1809.

[48] A. Fiala, C. Slagle, N. Legband, F. Aghabaglou, K. Buesing, M. Borden, et al., Treatment of a rat model of LPS-induced ARDS via peritoneal perfusion of oxygen microbubbles, J. Surg. Res. 246 (2020) 450–456, https://doi.org/10.1016/j.jss.2019.09.017.

[49] S.H. Mei, S.D. McCarter, Y. Deng, C.H. Parker, W.C. Liles, D.J. Stewart, Prevention of LPS-induced acute lung injury in mice by mesenchymal stem cells overexpressing angiopoietin 1, PLoS Med. 4 (9) (2007) e269, https://doi.org/10.1371/journal.pmed.0040269.

[50] W.A. Gathier, D.J. van Ginkel, M. van der Naald, F.J. van Slochteren, P.A. Doevendans, S.A.J. Chamuleau, Retrograde coronary venous infusion as a delivery strategy in regenerative cardiac therapy: an overview of preclinical and clinical data, J Cardiovasc Transl Res 11 (3) (2018) 173–181, https://doi.org/10.1007/s12265-018-9785-1.

[51] X. Zhang, X. Wei, Y. Deng, X. Yuan, J. Shi, W. Huang, et al., Mesenchymal stromal cells alleviate acute respiratory distress syndrome through the cholinergic anti-inflammatory pathway, Signal Transduct. Targeted Ther. 7 (1) (2022) 307, https://doi.org/10.1038/s41392-022-01124-6.

[52] D.S. Dzhalilova, A.M. Kosyreva, M.E. Diatroptov, E.A. Ponomarenko, I.S. Tsvetkov, N.A. Zolotova, et al., Dependence of the severity of the systemic inflammatory response on resistance to hypoxia in male Wistar rats, J. Inflamm. Res. 12 (2019) 73–86, https://doi.org/10.2147/JIR.S194581.

[53] M. Yamada, H. Kubo, S. Kobayashi, K. Ishizawa, M. He, T. Suzuki, et al., The increase in surface CXCR4 expression on lung extravascular neutrophils and its effects on neutrophils during endotoxin-induced lung injury, Cell. Mol. Immunol. 8 (4) (2011) 305–314, https://doi.org/10.1038/cmi.2011.8.

[54] S. Parasuraman, R. Raveendran, R. Kesavan, Blood sample collection in small laboratory animals, J. Pharmacol. Pharmacother. 1 (2) (2010) 87–93, https://doi.org/10.4103/0976-500X.72350.

[55] M.W. Pfaffl, A new mathematical model for relative quantification in real-time RT-PCR, Nucleic Acids Res. 29 (9) (2001) 45, https://doi.org/10.1093/nar/29.9.e45.

[56] A. Kosyreva, D. Dzhalilova, O. Makarova, I. Tsvetkov, N. Zolotova, M. Diatroptova, et al., Sex differences of inflammatory and immune response in pups of Wistar rats with SIRS, Sci. Rep. 10 (1) (2020), 15884, https://doi.org/10.1038/s41598-020-72537-y.

[57] A. Varin, S. Mukhopadhyay, G. Herbein, S. Gordon, Alternative activation of macrophages by IL-4 impairs phagocytosis of pathogens but potentiates microbial-induced signalling and cytokine secretion, Blood 115 (2) (2010) 353–362, https://doi.org/10.1182/blood-2009-08-236711.

[58] M.Ö. Celik, D. Labuz, J. Keye, R. Glauben, H. Machelska, IL-4 induces M2 macrophages to produce sustained analgesia via opioids, JCI insight 5 (4) (2020), e133093, https://doi.org/10.1172/jci.insight.133093.

[59] Y. Shintani, T. Ito, L. Fields, M. Shiraishi, Y. Ichihara, N. Sato, et al., IL-4 as a repurposed biological drug for myocardial infarction through augmentation of reparative cardiac macrophages: proof-of-concept data in mice, Sci. Rep. 7 (1) (2017) 6877, https://doi.org/10.1038/s41598-017-07328-z.

[60] D.R. Balce, B. Li, E.R. Allan, J.M. Rybicka, R.M. Krohn, R.M. Yates, Alternative activation of macrophages by IL-4 enhances the proteolytic capacity of their phagosomes through synergistic mechanisms, Blood, The Journal of the American Society of Hematology 118 (15) (2011) 4199–4208, https://doi.org/10.1182/blood-2011-01-328906.

[61] M. Rath, I. Müller, P. Kropf, E.I. Closs, M. Munder, Metabolism via arginase or nitric oxide synthase: two competing arginine pathways in macrophages, Front. Immunol. 5 (2014) 532, https://doi.org/10.3389/fimmu.2014.00532.

[62] Z. Yang, X.F. Ming, Functions of arginase isoforms in macrophage inflammatory responses: impact on cardiovascular diseases and metabolic disorders, Front. Immunol. 5 (2014) 533, https://doi.org/10.3389/fimmu.2014.00533.

[63] K.E. Sheldon, H. Shandilya, D. Kepka-Lenhart, M. Poljakovic, A. Ghosh, S.M. Morris Jr., Shaping the murine macrophage phenotype: IL-4 and cyclic AMP synergistically activate the arginase I promoter, J. Immunol. 191 (5) (2013) 2290–2298, https://doi.org/10.4049/jimmunol.1202102.

[64] I.M. Corraliza, G. Soler, K. Eichmann, M. Modolell, Arginase induction by suppressors of nitric oxide synthesis (IL-4, IL-10 and PGE2) in murine bone-marrow-derived macrophages, Biochem. Biophys. Res. Commun. 206 (2) (1995) 667–673, https://doi.org/10.1006/bbrc.1995.1094.

[65] D.R. Herbert, T. Orekov, A. Roloson, M. Ilies, C. Perkins, W. O'Brien, et al., Arginase I suppresses IL-12/IL-23p40-driven intestinal inflammation during acute schistosomiasis, J. Immunol. 184 (11) (2010) 6438–6446, https://doi.org/10.4049/jimmunol.0902009.

[66] B. Shu, Y. Feng, Y. Gui, Q. Lu, W. Wei, X. Xue, et al., Blockade of CD38 diminishes lipopolysaccharide-induced macrophage classical activation and acute kidney injury involving NF-κb signaling suppression, Cell. Signal. 42 (2018) 249–258, https://doi.org/10.1016/j.cellsig.2017.10.014.

[67] F. Morandi, I. Airoldi, D. Marimpietri, C. Bracci, A.C. Faini, R. Gramignoli, CD38, a receptor with multifunctional activities: from modulatory functions on regulatory cell subsets and extracellular vesicles, to a target for therapeutic strategies, Cells 8 (12) (2019) 1527, https://doi.org/10.3390/cells8121527.

[68] W. Li, Y. Li, X. Jin, Q. Liao, Z. Chen, H. Peng, et al., CD38: a significant regulator of macrophage function, Front. Oncol. 12 (2022), 775649, https://doi.org/10.3389/fonc.2022.775649.

[69] B. Shu, Y. Fang, W. He, J. Yang, C. Dai, Identification of macrophage-related candidate genes in lupus nephritis using bioinformatics analysis, Cell. Signal. 46 (2018) 43–51, https://doi.org/10.1016/j.cellsig.2018.02.006.

[70] J.A. Dewhurst, S. Lea, E. Hardaker, J.V. Dungwa, A.K. Ravi, D. Singh, Characterisation of lung macrophage subpopulations in COPD patients and controls, Sci. Rep. 7 (2017) 7143, https://doi.org/10.1038/s41598-017-07101-2.

[71] M. Fabbiani, A. Muscatello, P. Perseghin, M. Bani, A. Incontri, N. Squillace, et al., Brief report: peripheral monocyte/macrophage phenotypes associated with the evolution of cognitive performance in HIV-infected patients, J. Acquir. Immune Defic. Syndr. 76 (2017) 219–224, https://doi.org/10.1097/QAI.0000000000001480.

[72] J.H. Lam, H.H.M. Ng, C.J. Lim, X.N. Sim, F. Malavasi, H. Li, et al., Expression of CD38 on macrophages predicts improved prognosis in hepatocellular carcinoma, Front. Immunol. 10 (2019) 2093, https://doi.org/10.3389/fimmu.2019.02093.

[73] A.K. Azad, M.V. Rajaram, L.S. Schlesinger, Exploitation of the macrophage mannose receptor (CD206) in infectious disease diagnostics and therapeutics, J. Cytol. Mol. Biol. 1 (1) (2014), 1000003, https://doi.org/10.13188/2325-4653.1000003.

[74] R. Lucas, I. Czikora, S. Sridhar, E.A. Zemskov, A. Oseghale, S. Circo, et al., Arginase 1: an unexpected mediator of pulmonary capillary barrier dysfunction in models of acute lung injury, Front. Immunol. 4 (2013) 228, https://doi.org/10.3389/fimmu.2013.00228.

[75] H. Maarsingh, B.G. Dekkers, A.B. Zuidhof, I.S. Bos, M.H. Menzen, T. Klein, et al., Increased arginase activity contributes to airway remodelling in chronic allergic asthma, Eur. Respir. J. 38 (2) (2011) 318–328, https://doi.org/10.1183/09031936.00057710 74.

[76] R. Lucas, G. Yang, B.A. Gorshkov, E.A. Zemskov, S. Sridhar, N.S. Umapathy, et al., Protein kinase C-α and arginase I mediate pneumolysin-induced pulmonary endothelial hyperpermeability, Am. J. Respir. Cell Mol. Biol. 47 (4) (2012) 445–453, https://doi.org/10.1165/rcmb.2011-0332OC.

[77] H. Specht, E. Emmott, A.A. Petelski, R.G. Huffman, D.H. Perlman, M. Serra, et al., Single-cell proteomic and transcriptomic analysis of macrophage heterogeneity using SCoPE2, Genome Biol. 22 (1) (2021) 50, https://doi.org/10.1186/s13059-021-02267-5.

[78] C. O'Carroll, A. Fagan, F. Shanahan, R.J. Carmody, Identification of a unique hybrid macrophage-polarization state following recovery from lipopolysaccharide tolerance, J. Immunol. 192 (2014) 427–436, https://doi.org/10.4049/jimmunol.1301722.

[79] A. Boucher, N. Klopfenstein, W.M. Hallas, J. Skibbe, A. Appert, S.H. Jang, et al., The miR-23ã27ã24-2 microRNA cluster promotes inflammatory polarization of macrophages, J. Immunol. 206 (3) (2021) 540–553, https://doi.org/10.4049/jimmunol.1901277, 1.

[80] M. Moradi-Chaleshtori, M. Bandehpour, S. Soudi, S. Mohammadi-Yeganeh, S.M. Hashemi, In vitro and in vivo evaluation of anti-tumoral effect of M1 phenotype induction in macrophages by miR-130 and miR-33 containing exosomes, Cancer Immunol. Immunother. 70 (5) (2021) 1323–1339, https://doi.org/10.1007/s00262-020-02762-x.

[81] L. Li, G. Lv, B. Wang, L. Kuang, XIST/miR-376c-5p/OPN axis modulates the influence of proinflammatory M1 macrophages on osteoarthritis chondrocyte apoptosis, J. Cell. Physiol. 235 (2020) 281–293, https://doi.org/10.1002/jcp.28968.

[82] S.J. Yang, Y.Y. Chen, C.H. Hsu, C.W. Hsu, C.Y. Chang, J.R. Chang, et al., Activation of M1 macrophages in response to recombinant TB vaccines with enhanced antimycobacterial activity, Front. Immunol. 11 (2020) 1298, https://doi.org/10.3389/fimmu.2020.01298.

[83] E.M. Palmieri, M. Gonzalez-Cotto, W.A. Baseler, L.C. Davies, B. Ghesquière, N. Maio, et al., Nitric oxide orchestrates metabolic rewiring in M1 macrophages by targeting aconitase 2 and pyruvate dehydrogenase, Nat. Commun. 11 (2020) 1–17, https://doi.org/10.1038/s41467-020-14433-7.

[84] M. Yamashita, M. Niisato, Y. Kawasaki, S. Karaman, M.R. Robciuc, Y. Shibata, et al., VEGF-C/VEGFR-3 signalling in macrophages ameliorates acute lung injury, Eur. Respir. J. 59 (4) (2022), 2100880, https://doi.org/10.1183/13993003.00880-2021.

[85] S. Barratt, A.R. Medford, A.B. Millar, Vascular endothelial growth factor in acute lung injury and acute respiratory distress syndrome, Respiration 87 (4) (2014) 329–342, https://doi.org/10.1159/000356034.

[86] M.T. Kearns, S. Dalal, S.A. Horstmann, T.R. Richens, T. Tanaka, J.M. Doe, et al., Vascular endothelial growth factor enhances macrophage clearance of apoptotic cells, Am. J. Physiol. Lung Cell Mol. Physiol. 302 (7) (2012) 711–718, https://doi.org/10.1152/ajplung.00116.2011.

[87] R. Blondonnet, J.M. Constantin, V. Sapin, M. Jabaudon, A pathophysiologic approach to biomarkers in acute respiratory distress syndrome, Dis. Markers 2016 (2016), 3501373, https://doi.org/10.1155/2016/3501373.

[88] J.M. Forel, C. Guervilly, C. Farnarier, S.Y. Donati, S. Hraiech, N. Persico, et al., Transforming Growth Factor-β1 in predicting early lung fibroproliferation in patients with acute respiratory distress syndrome, PLoS One 13 (11) (2018), 0206105, https://doi.org/10.1371/journal.pone.0206105.

[89] O. Bottasso, M.V. Delpino, J. Quarleri, SARS-CoV-2 pathogenesis: imbalance in the renin-angiotensin system favors lung fibrosis, Front. Cell. Infect. Microbiol. 1 (2020) 340, https://doi.org/10.3389/fcimb.2020.00340.

[90] C.B. Vaz de Paula, S. Nagashima, V. Liberalesso, M. Collete, F.P.G. da Silva, A.G.G. Oricil, et al., COVID-19: immunohistochemical analysis of TGF-β signaling pathways in pulmonary fibrosis, Int. J. Mol. Sci. 23 (1) (2021) 168, https://doi.org/10.3390/ijms23010168.

[91] L. Zhu, X. Fu, X. Chen, X. Han, P. Dong, M2 macrophages induce EMT through the TGF-β/Smad2 signaling pathway, Cell Biol. Int. 41 (9) (2017) 960–968, 10.1002/cbin.10788.

[92] F. Liu, H. Qiu, M. Xue, S. Zhang, X. Zhang, J. Xu, et al., MSC-secreted TGF-β regulates lipopolysaccharide-stimulated macrophage M2-like polarization via the Akt/FoxO1 pathway, Stem Cell Res. Ther. 10 (1) (2019), 345, https://doi.org/10.1186/s13287-019-1447-y.

[93] A. Hariharan, A.R. Hakeem, S. Radhakrishnan, M.S. Reddy, M. Rela, The role and therapeutic potential of NF-kappa-B pathway in severe COVID-19 patients, Inflammopharmacology 29 (1) (2021) 91–100, https://doi.org/10.1007/s10787-020-00773-9.

[94] F. van de Veerdonk, M.G. Netea, Blocking IL-1 to prevent respiratory failure in COVID-19, Crit. Care 24 (2020) 445, https://doi.org/10.1186/s13054-020-03166-0.

[95] N.F. Wang, C.X. Bai, Bone marrow-derived mesenchymal stem cells modulate autophagy in Raw264.7 macrophages via the phosphoinositide 3-Kinase/Protein kinase B/Heme oxygenase-1 signaling pathway under oxygen-glucose Deprivation/Restoration conditions, Chin. Med. J. 134 (6) (2021) 699–707, https://doi.org/10.1097/cm9.0000000000001133.

[96] X. Liu, C. Gao, Y. Wang, L. Niu, S. Jiang, S. Pan, Bmsc-derived exosomes ameliorate lps-induced acute lung injury by mir-384-5p-Controlled alveolar macrophage autophagy, Oxid. Med. Cell. Longev. 2021 (2021), 9973457, https://doi.org/10.1155/2021/9973457.

[97] H. Qin, A. Zhao, Mesenchymal stem cell therapy for acute respiratory distress syndrome: from basic to clinics, Protein & cell 11 (10) (2020) 707–722, https://doi.org/10.1007/s13238-020-00738-2.

[98] S.M. Chacko, S. Ahmed, K. Selvendiran, M.L. Kuppusamy, M. Khan, P. Kuppusamy, Hypoxic preconditioning induces the expression of prosurvival and proangiogenic markers in mesenchymal stem cells, Am. J. Physiol. Cell Physiol. 299 (2010) C1562–C1570, https://doi.org/10.1152/ajpcell.00221.2010.

[99] Y.W. Lan, K.B. Choo, C.M. Chen, T.H. Hung, Y.B. Chen, C.H. Hsieh, et al., Hypoxia-preconditioned mesenchymal stem cells attenuate bleomycin-induced pulmonary fibrosis, Stem Cell Res. Ther. 6 (2015) 97, https://doi.org/10.1186/s13287-015-0081-6.

[100] W. Zhang, L. Liu, Y. Huo, Y. Yang, Y. Wang, Hypoxia-pretreated human MSCs attenuate acute kidney injury through enhanced angiogenic and antioxidative capacities, BioMed Res. Int. 2014 (2014), 462472, https://doi.org/10.1155/2014/462472.

[101] Y.Y. Wang, X.Z. Li, L.B. Wang, Therapeutic implications of mesenchymal stem cells in acute lung injury/acute respiratory distress syndrome, Stem Cell Res. Ther. 4 (2013) 45, https://doi.org/10.1186/scrt193.

[102] M.L. Bustos, L. Huleihel, E.M. Meyer, A.D. Donnenberg, V.S. Donnenberg, J.D. Sciurba, et al., Activation of human mesenchymal stem cells impacts their therapeutic abilities in lung injury by increasing interleukin (IL)-10 and IL-1RN levels, Stem Cells Transl Med 2 (11) (2013) 884–895, https://doi.org/10.5966/sctm.2013-0033.

[103] D. Li, Q. Liu, L. Qi, X. Dai, H. Liu, Y. Wang, Low levels of TGF-β1 enhance human umbilical cord-derived mesenchymal stem cell fibronectin production and extend survival time in a rat model of lipopolysaccharide-induced acute lung injury, Mol. Med. Rep. 14 (2) (2016) 1681–1692, https://doi.org/10.3892/mmr.2016.5416.

[104] M. Zoulikha, Q. Xiao, G.F. Boafo, M.A. Sallam, Z. Chen, W. He, Pulmonary delivery of siRNA against acute lung injury/acute respiratory distress syndrome, Acta Pharm. Sin. B 12 (2) (2022) 600–620, https://doi.org/10.1016/j.apsb.2021.08.009.

[105] R. Kandil, O.M. Merkel, Pulmonary delivery of siRNA as a novel treatment for lung diseases, Ther. Deliv. 10 (4) (2019) 203–206, https://doi.org/10.4155/tde-2019-0009.
[106] Q. Chen, M. Gao, Z. Li, Y. Xiao, X. Bai, K.O. Boakye-Yiadom, et al., Biodegradable nanoparticles decorated with different carbohydrates for efficient macrophage-targeted gene therapy, J. Contr. Release 323 (2020) 179–190, https://doi.org/10.1016/j.jconrel.2020.03.044.
[107] H. Xiao, Y. Guo, B. Li, X. Li, Y. Wang, S. Han, et al., M2-Like tumor-associated macrophage-targeted codelivery of STAT6 inhibitor and IKKβ siRNA induces M2-to-M1 repolarization for cancer immunotherapy with low immune side effects, ACS Cent. Sci. 6 (7) (2020) 1208–1222, https://doi.org/10.1021/acscentsci.9b01235.
[108] M.J. Khan, P. Singh, R. Dohare, R. Jha, A.H. Rahmani, S.A. Almatroodi, et al., Inhibition of miRNA-34a promotes M2 macrophage polarization and improves LPS-induced lung injury by targeting Klf4, Genes 11 (9) (2020) 966, https://doi.org/10.3390/genes11090966.
[109] L. Li, M. Qu, L. Yang, J. Liu, Q. Wang, P. Zhong, et al., Effects of ultrashort wave therapy on inflammation and macrophage polarization after acute lung injury in rats, Bioelectromagnetics 42 (6) (2021) 464–472, https://doi.org/10.1002/bem.22353.
[110] J.G. Laffey, M.A. Matthay, Fifty years of research in ARDS. Cell-Based therapy for acute respiratory distress syndrome. Biology and potential therapeutic value, Am. J. Respir. Crit. Care Med. 196 (3) (2017) 266–273, https://doi.org/10.1164/rccm.201701-0107CP.
[111] M.L. Bustos, L. Huleihel, M.G. Kapetanaki, C.L. Lino-Cardenas, L. Mroz, B.M. Ellis, et al., Aging mesenchymal stem cells fail to protect because of impaired migration and antiinflammatory response, Am. J. Respir. Crit. Care Med. 189 (7) (2014) 787–798, https://doi.org/10.1164/rccm.201306-1043OC.
[112] R.H. Lee, J.M. Yu, A.M. Foskett, G. Peltier, J.C. Reneau, N. Bazhanov, J.Y. Oh, D.J. Prockop, TSG-6 as a biomarker to predict efficacy of human mesenchymal stem/progenitor cells (hMSCs) in modulating sterile inflammation in vivo, Proc. Natl. Acad. Sci. U.S.A. 111 (47) (2014) 16766–16771, https://doi.org/10.1073/pnas.1416121111.
[113] Y. Liu, X. Tang, J. McArthur, J. Scott, S. Gartner, Analysis of human immunodežciency virus type 1 evidence for monocyte trafžcking into, Brain 6 (1) (2000) S70–S81.
[114] T. Fischer-Smith, J. Rappaport, Evolving paradigms in the pathogenesis of HIV-1-associated dementia, Expet Rev. Mol. Med. 7 (2005) 1–26, https://doi.org/10.1017/S1462399405010239.
[115] G. Herbein, A. Varin, The macrophage in HIV-1 infection: from activation to deactivation? Retrovirology 7 (2010) 33, https://doi.org/10.1186/1742-4690-7-33.
[116] J. Wilkinson, M. Radkowski, J.M. Eschbacher, T. Laskus, Activation of brain macrophages/microglia cells in hepatitis C infection, Gut 59 (2010) 1394–1400, https://doi.org/10.1136/gut.2009.199356.
[117] E.V. Stevenson, D. Collins-McMillen, J.H. Kim, S.J. Cieply, G.L. Bentz, A.D. Yurochko, Hcmv reprogramming of infected monocyte survival and differentiation: a goldilocks phenomenon, Viruses 6 (2014) 782–807, https://doi.org/10.3390/v6020782.
[118] K. Dutta, M.K. Mishra, A. Nazmi, K.L. Kumawat, A. Basu, Minocycline differentially modulates macrophage mediated peripheral immune response following Japanese encephalitis virus infection, Immunobiology 215 (2010) 884–893, https://doi.org/10.1016/j.imbio.2009.12.003.
[119] M.W. Sjoding, C.R. Cooke, T.J. Iwashyna, T.P. Hofer, Potential Effect on Clinical Study Results. Acute respiratory distress syndrome measurement error, Ann Am Thorac Soc 13 (7) (2016) 1123–1128, https://doi.org/10.1513/AnnalsATS.201601-072OC.
[120] X. Gao, Y. Mi, N. Guo, H. Xu, L. Xu, X. Gou, et al., Cytokine-induced killer cells as pharmacological tools for cancer immunotherapy, Front. Immunol. 8 (2017) 774, https://doi.org/10.3389/fimmu.2017.00774.